

## Article

# What Is Needed of a Scalar Field If It Is to Unify Inflation and Late Time Acceleration?

Nur Jaman <sup>1,2,\*</sup>  and Mohammad Sami <sup>1,3</sup>

<sup>1</sup> Centre for Cosmology and Science Popularization (CCSP), SGT University, Gurugram 122505, India; samijamia@gmail.com

<sup>2</sup> Indian Institute of Science Education and Research Kolkata, Mohanpur 741246, India

<sup>3</sup> Center for Theoretical Physics, Eurasian National University, Astana 010008, Kazakhstan

\* Correspondence: nurjaman@ctp-jamia.res.in

**Abstract:** Quintessential inflation refers to scenarios in which a single scalar field is used to describe inflation and late time acceleration. This review is dedicated to the framework of quintessential inflation, with a focus on the building blocks of formalism. Consistent unification of inflation and late time acceleration using a single scalar field asks for a shallow field potential initially followed by steep behaviour thereafter and shallow again around the present epoch. The requirement of non-interference of the scalar field with thermal history dictates the steep nature of potential in the post-inflationary era, with a further restriction that late time physics be independent of initial conditions. We describe, in detail, the scaling and asymptotic scaling solutions and the mechanism of exit from the scaling regime to late time acceleration. The review includes a fresh look at scaling solutions that are central to the theme of unification of inflation and late time acceleration. As for the exit mechanism, special attention is paid to the coupling of massive neutrino matter to the scalar field, which builds up dynamically and can give rise to late time acceleration. We present a detailed analytical treatment of scalar field dynamics in the presence of coupling. We briefly discuss the distinguishing feature of quintessential inflation, namely the blue spectrum of gravity waves produced during the transition from inflation to the kinetic regime.

**Keywords:** inflation; dark energy; scaling solution; exit mechanism; reheating; neutrino coupling



**Citation:** Jaman, N.; Sami, M. What Is Needed of a Scalar Field If It Is to Unify Inflation and Late Time Acceleration? *Galaxies* **2022**, *10*, 51. <https://doi.org/10.3390/galaxies10020051>

Academic Editor: Konstantinos Dimopoulos

Received: 15 February 2022

Accepted: 15 March 2022

Published: 23 March 2022

**Publisher's Note:** MDPI stays neutral with regard to jurisdictional claims in published maps and institutional affiliations.



**Copyright:** © 2022 by the authors. Licensee MDPI, Basel, Switzerland. This article is an open access article distributed under the terms and conditions of the Creative Commons Attribution (CC BY) license (<https://creativecommons.org/licenses/by/4.0/>).

## 1. Introduction

Accelerated expansion is generic to cosmological dynamics [1]. The Universe has gone through inflation [2–7] (for a review, see [8–11]) at early epochs and is accelerating at present [12,13]. Inflation addresses the logical inconsistencies of the hot big bang model and provides us with a mechanism for primordial perturbations believed to have grown via gravitational instability into the structure we see today in the Universe [7,14,15]. The age puzzle in the hot big bang necessitates late time acceleration [16,17] due to dark energy—cosmological constant, quintessence or large-scale modification of gravity. This phenomenon has been confirmed by direct as well as indirect observations [18,19], which, however, elude inflation. It is plausible to think that accelerated expansion is eternal, and that it had gone into hiding at an early epoch (end of inflation), allowing the thermal history to proceed as envisaged by the hot big bang, and it reappears today to account for the late time acceleration—re-incarnation of inflation. The term “Quintessential Inflation” refers to the paradigm of the unification of inflation and late time acceleration that does not disturb the thermal history [20–72]). In simple cases, inflation is driven by a scalar field, which, soon after the end of inflation, enters into an oscillatory phase and rapidly decays in particle species, giving rise to reheating/preheating of the Universe [65,73–99]). Attempts have been made to achieve the aforementioned goal by using a single scalar field as a source of both the phases of accelerated expansion in the framework of modified theories of gravity, particularly  $f(R)$  theories [61,100–104]. For instance, putting the Starobinsky proposal for

inflation and late time acceleration together using  $f(R)$  could suffice; see Ref. [105] on the related theme. In these models, it is difficult to eliminate the strong dependence on initial conditions. In this review, we shall focus on the scalar field models where one has better control on this problem.

At the onset, it sounds fairly straightforward to carry out the described unification in a single scalar field using a runaway type of potential that is shallow initially, suitable for slow roll, followed by steep behaviour for the entire history of the Universe and turning shallow again at late times to account for the observed acceleration. Though the presence of early and late time phases of accelerated expansion is evident in the proposal, nonetheless, remarks related to thermal history and the independence of late time evolution from initial conditions are in order. Since the potential is of the runaway type, the standard reheating mechanism is not operative in this framework. One needs to employ an alternative framework such as gravitational particle production [76,79] (see also [30]), instant preheating [62,65,84,90], curvaton preheating [85–87,89], Ricci reheating [106] (see also [107,108]) and so on. Radiation density produced in these processes at the end of inflation is smaller than the field energy density by several orders of magnitude. Due to the steep nature of potential in the post-inflationary era, the scalar field enters the kinetic regime soon after inflation ends ( $\rho_\phi \sim a^{-6}$ ) [109], such that radiation domination takes place after a long kinetic regime and field energy density becomes sub-dominant. There are two requirements for the field dynamics before it emerges from sub-dominance to dominance at late times: (1) it must adhere to the nucleosynthesis constraint; and (2) its emergence to late time acceleration must be unaffected by initial conditions. The latter puts a restriction on the class of field potentials that can be employed for quintessential inflation.

A comment on the duration of the kinetic regime is in order. The long kinetic regime might be problematic for nucleosynthesis due to relic gravity waves. Indeed, the energy density in relic gravity waves produced at the end of inflation increases in comparison to  $\rho_\phi$  during the kinetic regime and might conflict with the nucleosynthesis constraint at the commencement of the radiative regime. The nucleosynthesis constraint puts a lower bound on the reheating temperature at the end of inflation and an upper bound on the duration of the kinetic regime. One of the reheating alternatives is provided by gravitational particle production, which is a universal process that occurs due to a non-adiabatic change in space–time geometry when inflation ends; unlike other mechanisms, it does not require additional field(s); however, the nucleosynthesis bound is challenged. It should be noted that the presence of the kinetic epoch soon after the end of inflation induces a blue tilt in the gravitational wave spectrum. This feature enhances the prospects of detection of gravitational waves in the forthcoming observational missions. Further, a desirable feature of quintessential inflation should also be mentioned here; namely, the field should track the background in the post-inflationary era, and only at late times should it exit to acceleration. Several exit mechanisms have been analysed in the literature. We shall, however, focus on a particular one due to the coupling of the scalar field to massive neutrino matter. Last but not least, one should ask whether the unification scheme is an academic exercise or has a distinguished observational signature. The presence of the kinetic regime, a generic feature of quintessential inflation, induces a novel feature in the spectrum of relic gravity waves, namely the blue spectrum in the high-frequency regime. This is a generic model-independent prediction of the paradigm irrespective of its concrete realisation, to be tested in future observations (see Refs. [110,111] on the related theme).

This is a pedagogical review written specifically for young researchers. Efforts have gone into highlighting the general requirements and the corresponding building blocks of the paradigm, rather than discussing the technical details of concrete models of quintessential inflation. It goes without saying that the issues raised in the review are equally important for model building related to late time acceleration. We sincerely hope that the review will be helpful for beginners interested in related issues. The review should be read with the footnotes, which include additional explanations and clarifications. The organisation of the review is as follows. In Section 2, we describe broad features of the paradigm: a suitable

class of runaway potentials, alternative reheating models and exit mechanisms. In Section 3, we discuss the cosmological dynamics of the scalar field relevant to quintessential inflation. This includes field dynamics during the inflationary era, some model-independent features of inflation, the nucleosynthesis constraint and scaling and tracker behaviour in models of quintessential inflation. In Section 4, we describe a mechanism of exit from the scaling regime to late time acceleration, which is realised by invoking coupling to massive neutrino matter. In this section, the prospects for the detection of relic gravity waves are also discussed. Finally, we summarise the review in Section 4. We use the metric signature  $(-, +, +, +)$  and the notation for the reduced Planck mass,  $M_{\text{Pl}}^{-2} = 8\pi G$ .

## 2. Quintessential Inflation: Building Blocks

In this section, we broadly indicate the basic features of model building for quintessential inflation and list the building blocks of the model. Figure 1 shows the scalar field potential, flat at both the early and late time epochs and steep in between, joining the two ends. One immediate implication of the runaway type nature of the potential is the requirement for an alternative reheating mechanism. There are a few alternatives to be mentioned in the discussion to follow. It is important to note that in the context of warm inflation [112,113], a separate reheating mechanism may not be required as radiation is being produced during inflation itself due to the coupling of the inflaton field to the radiation bath. The idea of “warm inflation” also works in the context of quintessential inflation as well [99,114–117]. We shall also mention specific field tracks that could join the two phases of acceleration such that thermal history is left without interference and the late time physics is insensitive to initial conditions.

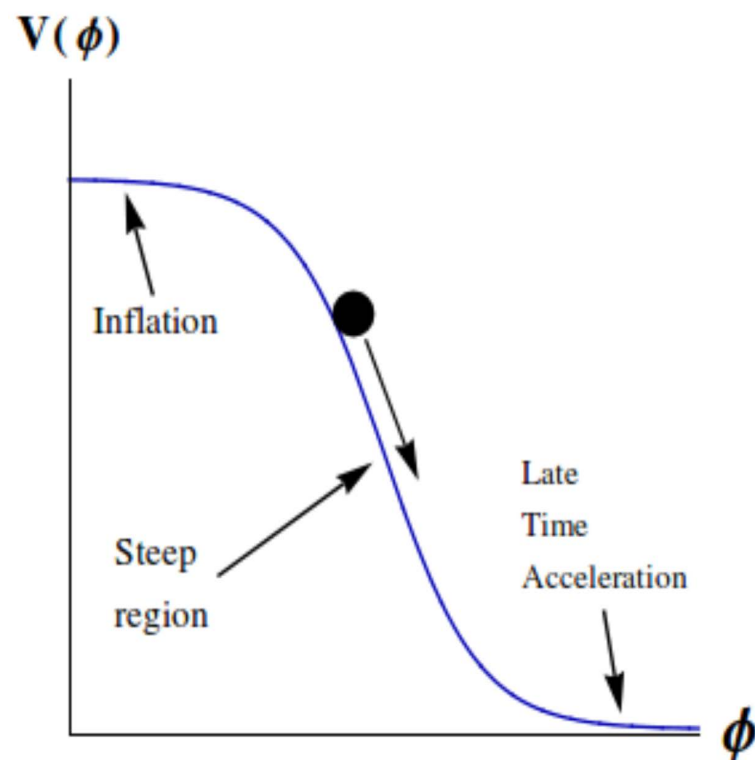


**Figure 1.** The figure displays a typical scalar field potential required to realise quintessential inflation: potential shallow initially, followed by steep behaviour thereafter, and shallow again around the present epoch.

### 2.1. Reheating through Gravitational Particle Production

Gravitational particle production takes place at the end of inflation due to a non-adiabatic change in space–time geometry [76] (see also [79]). It is a universal process and does not require the presence of additional field(s). The energy density of radiation produced in this

process is given by  $\rho_r \simeq 0.01 \times g_p H_{\text{end}}^4$ , where  $g_p \sim 100$ , the number of relativistic degrees produced in the process; it involves  $H_{\text{end}}$ , the natural scale available at the end of inflation. In this case, typically,  $\rho_\phi / \rho_r \simeq 10^{-10}$  [22], and the process is inefficient and might challenge the nucleosynthesis constraint due to the overproduction of relic gravity waves. Other alternatives include instant preheating, the curvaton reheating mechanism and Ricci reheating.

### 2.2. Instant Preheating

Instant preheating [84,90] operates with an assumption that the inflaton field  $\phi$  interacts with another scalar field  $\chi$  (with coupling  $g$ ) whose mass depends upon  $\phi$  such that as  $\phi$ , after inflation, runs down its potential,  $m_\chi$  increases and decays into matter fields<sup>1</sup> ( $\chi$  couples to matter fields with coupling  $h$ ). By appropriately choosing couplings ( $g, h < 1$ ), one can obtain instantaneous preheating at the end of inflation with the reheating temperature that satisfies the bound implied by the nucleosynthesis constraint.

### 2.3. Curvaton Reheating

The Lagrangian is supplemented with an extra field  $\sigma$  with a quadratic mass term of  $m_\sigma^2 \sigma^2$ , such that  $m_\sigma \ll H_{\text{inf}}$  and the  $\sigma$  field ceases to play any role during inflation [85–87,89]. After inflation ends, the Hubble parameter decreases  $m_\sigma \sim H$  and the  $\sigma$  field begins to oscillate and decay into matter fields, giving rise to reheating with the desired temperature at the end of inflation.

### 2.4. Ricci Reheating

The problem associated with gravitational reheating, i.e., overproduction of gravitational waves, can be controlled by introducing another reheating mechanism called Ricci reheating [106–108]. In this mechanism, a scalar field called a reheaton is non-minimally coupled directly with the Ricci scalar. The Ricci scalar changes sign after the end of inflation, when the kinetic energy takes over the potential in the steep region of the potential. As a result, the effective mass of the reheaton changes sign and becomes tachyonic. Due to the tachyonic nature, the reheaton field grows as the field rolls down towards new effective minima. The reheating is realised by the transfer of energy from this reheaton to standard model particles. It is also possible to identify a reheaton with the Higgs field [108].

### 2.5. Independence of Late Time Dynamics from Initial Conditions

The requirement of steep potential in the post-inflationary era is dictated by the need to achieve the commencement of radiation domination after which the scalar field remains sub-dominant. However, a specific type of steep behaviour is asked for, which allows the scalar field to follow the background—the *scaling solution*, which is an attractor of dynamical systems. The nucleosynthesis constraint, further, puts a lower bound on the slope of these potentials. Scaling behaviour, for instance, is exhibited by a steep exponential potential, ( $V \sim \text{Exp}(-\alpha\phi/M_{\text{Pl}}; \alpha^2 > 3)$ ) [118–121]. However, the scaling solution is non-accelerating as, in this case,  $w_\phi = w_b = (0, 1/3)$  for cold dark matter and radiation, respectively. Hence, in this case, one needs to invoke an additional feature in the potential that could trigger an exit to late time acceleration. Once the model parameters are set to exit to acceleration at the present epoch, changing the initial conditions within a reasonable range does not affect the late time physics *à la a tracker* [122,123].

### 2.6. Exit Mechanisms

There are several ways to realise the exit from the scaling regime to accelerated expansion. (1) One might simply add a cosmological constant to the scalar field Lagrangian or, if one is willing to go further, one might add to the scalar field potential a term,  $V_1 \sim \text{Exp}(-\lambda_1\phi/M_{\text{Pl}})$ ,  $\lambda_1^2 < 2$  [120,124,125], such that it becomes operative only at late times, giving rise to slow roll. (2) One might add to the Lagrangian a Gauss–Bonnet term coupled to the scalar field,  $\zeta(\phi)R_{\text{GB}}^2$  ( $R_{\text{GB}}^2 = R^2 - 4R_{\mu\nu}R^{\mu\nu} + R_{\mu\nu\alpha\beta}R^{\mu\nu\alpha\beta}$ ), which can induce a minimum in the runaway potential and might give rise to late time acceleration

by suitably choosing the coupling [126]. However, it might be difficult to make this term invisible during inflation. (3a) It is rather straightforward to induce a minimum in the scalar field potential by introducing the coupling of the scalar field to (cold) matter, which is proportional to the trace of the matter energy momentum tensor and vanishes identically during the radiation era [127]. In this case, the scalar field can settle in the minimum of the effective potential, giving rise to de Sitter-like behaviour, of interest to late time cosmology. However, this happens soon after matter domination is established, where it is undesirable as the matter phase should be left intact. (3b) This problem can be circumvented by invoking the coupling of the scalar field to massive neutrino matter, which builds up dynamically only at late times as massive neutrinos turn non-relativistic. In this paper, we shall focus on the dynamics of this process.

### 2.7. Suitable Class of Scalar Field Potentials

It is difficult to have a tractable analytical expression of a potential shallow initially as required by inflation with a tracker-like behaviour in the post-inflationary era. We often encounter the following classes of potentials in the literature. (a) Potentials that are steep initially with a desired behaviour thereafter—for instance, inverse power law potentials. The known way to have accelerated expansion in the initial phase in this case is provided by “Brane Worlds” [22,31,62,128], where high-energy Brane corrections can give rise to slow roll with a graceful exit to deceleration as the field runs down its potential and Brane damping disappears. Unfortunately, this scenario gives rise to a large tensor to scalar ratio of perturbations, which is ruled out by observation [129]. (b) A class of potentials that are flat initially, followed by a steep behaviour. For instance,  $V \sim \text{Exp}(-\lambda\phi^n / M_{\text{Pl}}^n)$ ,  $n > 1$  [130]. Potentials with this characteristic can also be constructed using a non-canonical form of the scalar field Lagrangian. In this case, one is required to invoke an exit mechanism to late time acceleration. (c) If we do not adhere to tracker-like behaviour in the post-inflationary era, it is possible to find a class of potentials that are shallow at early and late times and steep in between, with a *thawing realisation* [63].

## 3. Cosmological Dynamics of Scalar Field in a Nut Shell

Scalar field dynamics has played an important role in modern cosmology, starting with inflation, which led to a paradigm shift resulting in the integration of cosmology with high-energy physics. In what follows, we present the basic elements of scalar field dynamics with and without the presence of background matter. Our discussion revolves around scaling solutions and slow roll attractors. Special attention is paid to asymptotic scaling solutions, one of the important building blocks of quintessential inflation. However, since the scaling solutions are non-accelerating in nature, one requires mechanisms of exit to late time acceleration. We discuss in detail the exit caused by the coupling of the scalar field to massive neutrino matter. The generic coupling is proportional to the trace of the energy momentum tensor of massive neutrino matter, which vanishes as long as neutrinos are relativistic. Coupling acquires a non-zero value at late stages of evolution when neutrinos become non-relativistic. This is a unique physical process that occurred in the Universe, and neutrino mass is the only available energy scale close to the mass scale associated with dark energy (see, for review on dark energy, [131–138]; see also [139]). The coupling of the scalar field to massive neutrino matter invokes an important feature in the scalar field potential responsible for late time acceleration. We will include details in the sub-section to follow.

### 3.1. Field Evolution in Absence of Background Matter: Slow Roll versus Fast Roll

Scalar dynamics has been used extensively in the development of models for both inflation and late time acceleration. In this section, we shall focus on the dynamics of a

non-minimally coupled scalar field. Let us consider the action of a minimally coupled scalar field  $\phi$ , which populates the FLRW universe [136,140–142]:

$$\mathcal{S} = \int d^4x \sqrt{-g} \left[ \frac{M_{\text{Pl}}^2}{2} R + \mathcal{L}(\phi) \right] \equiv \int d^4x \sqrt{-g} \left[ \frac{M_{\text{Pl}}^2}{2} R - \frac{1}{2} \partial_\mu \phi \partial^\mu \phi - V(\phi) \right] \quad (1)$$

The energy momentum tensor for the scalar field reads

$$T_{\mu\nu}(\phi) = \partial_\mu \phi \partial_\nu \phi + g_{\mu\nu} \mathcal{L}(\phi) \quad (2)$$

such that the field energy density and pressure are given by

$$T^0_0 \equiv -\rho_\phi = \frac{1}{2} \dot{\phi}^2 + V(\phi); \quad T^i_i \equiv p_\phi = \frac{1}{2} \dot{\phi}^2 - V(\phi) \quad (3)$$

For the FLRW background dominated by the scalar field energy density, we have

$$\left( \frac{\dot{a}}{a} \right)^2 \equiv H^2 = \left( \frac{1}{3M_{\text{Pl}}^2} \right) \rho_\phi \quad (4)$$

$$-\frac{\dot{H}}{H^2} = \frac{3}{2}(1 + w_\phi) = 3 \frac{\dot{\phi}^2/2}{\rho_\phi} \iff \frac{\ddot{a}}{a} = -\frac{1}{6M_{\text{Pl}}^2} \rho_\phi (1 + 3w_\phi) \quad (5)$$

where the equation of state parameter for the field is defined as

$$w_\phi \equiv \frac{P_\phi}{\rho_\phi} = \frac{\frac{1}{2} \dot{\phi}^2 - V(\phi)}{\frac{1}{2} \dot{\phi}^2 + V(\phi)}, \quad (6)$$

which interpolates between 1 and  $-1$ . The lower (upper) limit corresponds to the potential (kinetic) energy-dominated situation. The field configuration with  $w_\phi \simeq -1$  or  $-\frac{\dot{H}}{H^2} \ll 1$  is referred to (quasi) de Sitter, for which  $H$  is approximately constant and  $a(t) \sim e^{Ht}$ . In this case, the field rolls slowly,

$$\dot{\phi}^2/2 \ll V(\phi) \implies \epsilon \equiv 3 \frac{\dot{\phi}^2/2}{\rho_\phi} \simeq \frac{3}{2} \frac{\dot{\phi}^2}{V} \ll 1 \quad (7)$$

where  $\epsilon$  is one of the slow roll parameters. The (quasi) de Sitter configuration is admitted by the scalar field dynamics as a possible fixed point. Indeed, the scalar field equation that follows from (1) in the FLRW background is

$$\ddot{\phi} + 3H\dot{\phi} + V_\phi = 0; \quad V_\phi \equiv \frac{dV}{d\phi} \quad (8)$$

where the second term with the Hubble rate acts as a friction coefficient. Field Equation (8) is equivalent to energy conservation,

$$\dot{\rho}_\phi + 3H\rho_\phi(1 + w_\phi) = 0 \quad (9)$$

which formally integrates to

$$\rho_\phi = \rho_{in} e^{-3 \int (1+w_\phi) \frac{da}{a}}, \quad (10)$$

with  $\rho_{in}$  as a integration constant. For a potential energy-dominated situation,  $\dot{\phi}^2/2 \ll V$  ( $w_\phi \simeq -1$ ), and the field energy density is approximately constant, whereas in the opposite case ( $\dot{\phi}^2/2 \gg V$ ), dubbed the kinetic regime,  $\rho_\phi \sim 1/a^6$ . The kinetic regime is realised in the case of a steep potential where the field rolls down its potential rapidly, making the potential energy redundant and giving rise to  $\rho_\phi \sim a^{-6}$ .

As mentioned before, we are interested in realising the quasi de Sitter configuration. To this effect, we notice that when the friction term in Equation (8) is large,

$$\beta \equiv -\frac{\ddot{\phi}}{3H\dot{\phi}} \ll 1 \implies \text{Slow roll regime : } 3H\dot{\phi} + V_{\phi} \simeq 0; \quad H^2 \simeq \frac{1}{3M_{Pl}^2} V(\phi) \quad (11)$$

where  $\dot{\phi}$  is small and adheres to the slow roll condition, namely  $\epsilon \ll 1$ , which in turn implies that the potential is nearly flat<sup>3</sup>

$$\epsilon = \frac{M_{Pl}^2}{2} \left( \frac{V_{\phi}}{V} \right)^2 \quad (12)$$

In this case, even if we begin with a huge acceleration,  $\ddot{\phi}$ , it is taken care of by the friction term. Thus, the slow roll dynamics confirms the existence of a (quasi) de Sitter fixed point, also known as the slow roll solution. We should, however, check the consistency of (11) with the field Equation (8). Taking the time derivative of slow roll Equation (11) and using Equation (5), we have

$$\beta = -\frac{\ddot{\phi}}{3H\dot{\phi}} = +\frac{V_{\phi\phi}}{9H^2} - \frac{(1+w_{\phi})}{2}; \quad V_{\phi\phi} = \frac{d^2V}{d\phi^2} \quad (13)$$

Keeping  $\beta$  negligible requires

$$\epsilon = \frac{M_{Pl}^2}{2} \left( \frac{V_{\phi}}{V} \right)^2 \ll 1 \quad (14)$$

$$\eta = M_{Pl}^2 \frac{V_{\phi\phi}}{V} \ll 1, \quad (15)$$

which express the self-consistency of slow roll approximation with full scalar field dynamics. Thus, we are hereby led to two necessary conditions for slow roll. The first condition tells us that the slope of the potential small and potential is shallow ( $M_{Pl}|V_{\phi}/V| \ll 1$ ), whereas the second condition is a statement about the smallness of the curvature, which ensures that slow roll can be sustained for the long duration ( $\dot{\epsilon}/H\epsilon = \mathcal{O}(\eta, \epsilon)$ ) needed to collect the required number of e-foldings necessary to address the shortcomings of the hot big bang model. The smallness of  $\eta$  is also dictated by the flatness of the perturbation spectrum. Thus, the smallness of slow roll parameters ensures the required number of e-foldings and the scale-independent spectrum of adiabatic density perturbations produced during inflation.

### 3.2. Inflation: Model-Independent Features

As mentioned before, we focus on generic features of the paradigm rather than the concrete models. In what follows, we present the model-independent estimates of inflation to be used later. We recall that the tensor-to-scalar ratio,  $r$ , is defined as the ratio of amplitudes of the tensor and scalar perturbations,

$$r \equiv \frac{P_T}{P_S} \quad (16)$$

which is expressed through  $\epsilon$  in the case of a canonical scalar field as  $r = 16\epsilon$ . Observations [143] put a bound on the tensor-to-scalar ratio of perturbations, namely  $r \lesssim 0.032$  [144], which translates into a restriction on the slope of the potential,  $\lambda_s \equiv -M_{Pl} \frac{V_{,\phi}}{V} \lesssim 0.06$ , which is a tighter bound on the slope than the one imposed by the slow roll condition. The scalar power spectrum,

$$P_S = \frac{1}{8\pi^2} \frac{1}{\epsilon} \frac{H^2}{M_{Pl}^2} \Big|_{k=aH} = \frac{2}{\pi} \frac{1}{r} \frac{H_{\text{inf}}^2}{M_{Pl}^2} \quad (17)$$

is bound due to CMB observations and adhering to recent findings [143,144], we have  $H_{\text{inf}} \simeq 5.8 \times 10^{-5} r^{1/2} M_{\text{Pl}} = 1.4 \times 10^{14} r^{1/2} \text{ GeV}$ , or, equivalently,  $V_{\text{inf}}^{1/4} = 0.01 \times r^{1/2} M_{\text{Pl}}$ . At the end of inflation,  $\epsilon = 1$ , which implies that  $\dot{\phi}_{\text{end}} = V_{\text{end}}^{1/2}$ , and we have the Hubble parameter at the end of inflation:

$$H_{\text{end}} = \frac{1}{\sqrt{2} M_{\text{Pl}}} V_{\text{end}}^{1/2}. \quad (18)$$

Since inflation is a quasi de Sitter phase of expansion, it is expected that  $H$  does not change much from commencement to the end of inflation. The argument is supported by the observational upper bound on the tensor-to-scalar ratio  $r \lesssim 0.032$ , such that the field excursion during inflation is not significant. This is supported by numerical calculation for generalised exponential potential, which shows that not only  $H_{\text{inf}} \& H_{\text{end}}$  but  $H_{\text{inf}}, H_{\text{end}} \& H_{\text{kin}}$  are within the same order of magnitude [56].

Using Equation (18), we have the estimation for  $V_{\text{end}}$ :

$$V_{\text{end}} \approx 2H_{\text{inf}}^2 M_{\text{Pl}}^2 \Rightarrow \rho_{\phi, \text{end}} = \frac{3}{2} V_{\text{end}} \approx 3H_{\text{inf}}^2 M_{\text{Pl}}^2 \quad (19)$$

In the kinetic epoch followed by inflation, the energy densities of the field and radiation evolve as follows:

$$\rho_{\phi} = \rho_{\phi, \text{end}} \left( \frac{a_{\text{end}}}{a} \right)^6 \quad (20)$$

$$\rho_r = \rho_{r, \text{end}} \left( \frac{a_{\text{end}}}{a} \right)^4 \quad (21)$$

Thus, the ratio of the scale factors at the end of inflation to the commencement of the radiation epoch or that of the respective temperatures are obtained by using  $\rho_{\phi}(a_r) = \rho_r(a_r)$ , which gives

$$\frac{a_r}{a_{\text{end}}} = \frac{T_{\text{end}}}{T_r} = \left[ \frac{\rho_{\phi, \text{end}}}{\rho_{r, \text{end}}} \right]^{1/2}. \quad (22)$$

The length of the kinetic regime depends upon the ratio of field energy density to the radiation energy density at the end of inflation. An efficient reheating process implies a smaller value of this ratio, corresponding to a shorter kinetic regime. Owing to the steep nature of the scalar field potential in the post-inflationary era, the field runs down its potential rapidly after inflation ends and, in a short time, enters the kinetics. In fact, it is found numerically that, for the potential (69),  $H_{\text{inf}}, H_{\text{end}}$  and  $H_{\text{kin}}$  are within the same order of magnitude [56]. We shall use  $H_{\text{inf}} \simeq H_{\text{end}} \simeq H_{\text{kin}}$  in our estimations for model-independent predictions.

### 3.3. Evolution in Presence of Background Matter: Scaling Solution

Scalar field dynamics in the presence of background matter (cold matter/radiation) exhibits distinguished features. Under specific conditions, the scalar field might mimic the background matter *à la* the *scaling solution*, which plays an important role in model building for dark energy and quintessential inflation. In order to check for the scaling behaviour of  $\rho_{\phi}$ , let us consider evolution equations in the presence of background matter [120,136,141,145,146].

$$H^2 = \frac{1}{3M_{\text{Pl}}^2} (\rho_b + \rho_{\phi}) \quad (23)$$

$$\dot{H} = -\frac{1}{2M_{\text{Pl}}^2} \left( (1 + w_B) \rho_b + \dot{\phi}^2 \right) \quad (24)$$

$$\dot{\rho}_b + 3H\rho_b(1 + w_b) = 0 \quad (25)$$

where  $\rho_b$  and  $w_b$  designate the energy density and equation of state parameter for background matter, respectively. As for the scalar field equation, background dependence is reflected there through the Hubble parameter. It follows from the continuity equation for background matter that  $\rho_B \sim a^{-3(1+w_b)}$ . The scaling solution is defined requiring that the scalar field evolves exactly as the background matter:

$$\text{Scaling solution : } w_\phi = w_b; \rho_\phi \sim a^{-3(1+w_b)} \quad (26)$$

The scaling solution is a specific dynamical arrangement that preserves the ratio of kinetic to potential energy of the field,

$$w_\phi \equiv \frac{P_\phi}{\rho_\phi} = \frac{\frac{1}{2}\dot{\phi}^2 - V(\phi)}{\frac{1}{2}\dot{\phi}^2 + V(\phi)} = w_b \Rightarrow \dot{\phi}^2(1 - w_b) = 2V(1 + w_b) \quad (27)$$

We recall from earlier discussion that the interplay between the friction term and the gradient of potential reflects the nature of the solution of the field equation; the scaling solution should impose certain restrictions on their ratio. Indeed, differentiating (27) left right and using the field Equation (8), we have

$$(3H\dot{\phi} + V_\phi)\dot{\phi}(1 - w_b) = -(1 + w_b)V_\phi\dot{\phi} \Rightarrow -3(1 - w_b)H\dot{\phi}^2 = 2V_\phi\dot{\phi} \quad (28)$$

Equations (27) and (28) yield two important properties of scaling solutions, namely [146]

$$X \equiv \frac{\dot{\phi}^2}{2V} = \frac{1 + w_b}{1 - w_b} \quad (29)$$

$$Y \equiv \frac{V_\phi}{\dot{\phi}H} = \frac{3}{2}(w - 1) \quad (30)$$

Let us also note that, for the scaling solution,

$$-\frac{\dot{H}}{H^2} = \frac{3}{2}(1 + w_b) \quad (31)$$

$$\frac{\ddot{\phi}}{\dot{\phi}H} = -\frac{3}{2}(1 + w_b). \quad (32)$$

These equations readily yield the behaviour of the scalar field in the scaling regime [125,146],

$$H(t) = \frac{1}{3(1 + w_b)t}; \dot{\phi} \propto t^{-1} \Rightarrow \phi(t) \propto \ln(t) \quad (33)$$

Thus far, we have not needed any information on the field potential that would support the scaling behaviour. It is interesting to compute the  $\Omega_\phi$  for the scaling solution that would tell us about the fraction of total energy that  $\rho_\phi$  constitutes and also the nature of the potential. Using Equations (29) and (30), we find

$$\Omega_\phi = \frac{\rho_\phi}{3M_{Pl}^2 H^2} = \frac{1}{3M_{Pl}^2} \left( \frac{XY^2}{1 - w_b} \right) \left( \frac{V}{V_\phi} \right)^2 = \frac{3(1 + w_b)}{4\lambda_s^2}; \lambda_s \equiv -M_{Pl} \frac{V_\phi}{V} \quad (34)$$

where  $\lambda_s$  is the slope of the potential. Since  $\rho_\phi$  scales as the energy density of background matter in the scaling regime,  $\Omega_\phi = Const$ , which in turn implies that the slope of the potential should be constant and, consequently, the exponential potential is singled out,

$$V(\phi) = V_0 e^{-\alpha\phi/M_{Pl}}; \lambda_s = \alpha \quad (35)$$

However, an important piece of information is yet missing in our analysis. For instance, if the slope is small, namely  $\alpha^2 < 2$ , the slow roll condition applies and we have  $w_\phi < -1/3 \rightarrow \dot{\phi}^2/2 < V/2$  and no scaling solution in this case. This brings us to the

question of the existence and stability of the scaling solutions we are interested in, which is addressed by dynamical analysis using the autonomous form of evolution equations. Using the following notations [120]<sup>4</sup>,

$$x \equiv \frac{\dot{\phi}}{\sqrt{6}M_{Pl}H}; \quad y \equiv \frac{\sqrt{V}}{\sqrt{3}M_{Pl}H'} \quad (36)$$

one can cast evolution equations, with exponential potential, in the autonomous form,

$$x' = f(x, y); \quad y' = g(x, y) \quad (37)$$

along with the Friedman constraint equation,

$$\frac{\rho_B}{3M_{Pl}^2H^2} + x^2 + y^2 = 1 \quad (38)$$

where prime denotes the derivative with respect to  $N \equiv \ln(a)$ ;  $f$  and  $g$  are functions of  $x$  and  $y$  whose functional forms are not required here. The fixed point of the dynamical system is the one for which  $x', y' = 0$ , whose stability is checked looking at the sign of the eigenvalues of the perturbed matrix. Using this analysis, one finds [120,125,145]

$$\text{Scaling solution :} \quad w_\phi = w_m; \quad \Omega_\phi = \frac{3(1+w_b)}{\alpha^2} \quad \lambda_s^2 = \alpha^2 > 3 \quad (39)$$

which is an attractor of the dynamical system and this completes the story. In the scaling regime,  $\rho_\phi$  constitutes a constant fraction of the total energy density. The fraction is smaller for the larger value of the slope of the potential. In fact, the lower bound on the slope is fixed by the nucleosynthesis constraint. Exponential potential with slope larger than  $\sqrt{3}$  is termed *steep*; otherwise, it is *shallow*, which also serves as a yardstick for an arbitrary potential. Let us note that a field-dominated solution ( $\Omega_\phi = 1$ ) is also an attractor for  $\alpha^2 < 3$ , which we are not interested in here. The demarcation is clear: for  $\alpha^2 > 3$ , the system settles into a scaling regime; otherwise, it is a field-dominated solution, which is accelerating if  $\alpha^2 < 2$ .

To summarise, the scaling solution follows the background matter being sub-dominant. During the radiation era, field energy density scales as radiation energy density ( $\rho_r$ ), namely  $\rho_\phi \sim a^{-4}$ , which adjusts itself to  $\rho_m$  (energy density of cold matter) after matter domination is established and follows it forever. The scaling regime is characterised by a fixed kinetic to potential energy ratio—for instance,  $\dot{\phi}^2/2 = V$  in the radiation era, whereas  $\dot{\phi}^2/2 = 2V$  for matter domination. Last but not least, since scaling solutions are non-accelerating, one requires an additional feature in the potential that would allow an exit to late time acceleration. In this framework,  $\Gamma = 1$  and  $w_\phi = w_b$  for most of the history of the Universe, and, only at late times, transition to acceleration would take place *à la a perfect tracker*. In the forthcoming discussion, we shall mention the exit mechanisms discussed in the literature.

### 3.4. Nucleosynthesis Constraint on Extra Species

One of the major successes of the hot big bang includes the synthesis of light elements, Deuterium ( $^2\text{H}$ ), Tritium ( $^3\text{H}$ ) and Helium ( $^4\text{He}$ ), in the early Universe. When the temperature in the Universe was around 1 TeV, all the standard model degrees of freedom were in equilibrium. All of them were relativistic and contributed to the radiation energy density [147,148],

$$\rho_r = \frac{\pi^2}{30} g_*(T) T^4 \quad (40)$$

where  $g_*(T)$  denotes the effective number of relativistic degrees of freedom in the Universe at temperature  $T$ . Relativistic species including both the bosons and the fermions contribute to  $g_*(T)$ ,

$$g_*(T) = \sum_{\text{Bosons}} g_B \left( \frac{T_i}{T} \right)^4 + \frac{7}{8} \sum_{\text{Fermions}} g_F \left( \frac{T_i}{T} \right)^4, \quad (41)$$

where  $T$  is the photon gas temperature and  $g_B$  and  $g_F$  denote bosonic and fermionic degrees of freedom with mass  $m_i \ll T$  ( $m_i$  is the mass of a particular species). The effective degrees of freedom are defined relative to the photon gas. When the temperature dropped to around  $1 \text{ MeV}$ , the relativistic species included  $\gamma, e, e^+$  and three generations of neutrinos  $\nu$  such that  $g_* = 10.75$ . Weak processes such as  $p + e^- \leftrightarrow n + \nu_e$  then froze out, leaving behind a definite ratio of  $n/p$  densities. Freezing temperature can be estimated comparing the reaction rate  $\Gamma_{int} = G_F^2 T_f^5$  with the Hubble parameter  $H(T)$  [149],

$$G_F^2 T_f^5 = \frac{g_*^{1/2}}{\sqrt{3} M_{\text{Pl}}} T_f^2 \Rightarrow T_f = \left( \frac{g_*^{1/2}}{\sqrt{3} G_F^2 M_{\text{Pl}}} \right)^{1/3} \simeq 1 \text{ MeV} \quad (42)$$

where  $G_F$  is the Fermi constant and  $T_f$  designates the freezing temperature. It should be noted that the  $n/p$  density ratio is temperature-sensitive, as  $n/p \sim \text{Exp}(-Q/T_f)$ , where  $Q$  denotes the neutron and proton mass difference. Since  $T_f$  is less than the binding energy of Deuterium, its synthesis should naively begin. However, there are more than a billion photons per proton ( $\eta = n_B/n_\gamma \simeq 6 \times 10^{-10}$ ,  $n_B$  designated baryon number density) in the Universe, such that the number of photons whose energy exceeds  $T_f$  is large and Deuterium does not form due to photo-dissociation. This process is delayed and occurs at a lower temperature,  $T_{BBN} \simeq 0.1 \text{ eV}$ , which then initiates the chain reaction for Helium formation. Helium abundance in the Universe has been measured accurately; it is sensitive to  $T_f$ , and for obvious reasons, it also depends upon  $\eta$ . We should emphasise that  $\eta$  is an important input here, required for a successful nucleosynthesis. It is further important to note that bringing in any extra relativistic degree of freedom such as a scalar field would affect the numerical value of  $T_f$  and consequently the Helium abundance. The latter should, therefore, impose a constraint on any relativistic degree of freedom in the Universe over and above the standard model of particle physics—the *nucleosynthesis constraint*—which, in particular, applies to often used quintessence as well as relic gravity waves. Indeed, for temperatures under consideration,

$$g_* = 2 + \frac{7}{8}(4 + 2N_\nu) \quad (43)$$

where the first term is due to a photon, and the first term in the brackets is attributed to an electron and positron;  $N_\nu = 3$  in the standard model. Any extra radiation present in the Universe can be parametrised through  $N_\nu$  [150]

$$\Delta\rho_r = \frac{\pi^2}{30} \frac{7}{4} \Delta N_\nu T^4 \quad (44)$$

where  $\Delta N_\nu$  is anything over and above the standard model value of  $N_\nu$  ( $N_\nu = 3$ ), which should be constrained from the observed primordial abundances and other data. Let us now assume an extra relativistic degree of freedom in the Universe dubbed “ $X$ ” with energy density  $\rho_X$ , which should not exceed  $\Delta\rho_r$  as a necessary requirement for not disturbing the Helium abundance [150],

$$\left( \frac{\rho_X}{\rho_\gamma} \right)_{1 \text{ MeV}} \leq \frac{7}{8} \Delta N_\nu \quad (45)$$

where  $\rho_\gamma = (\pi^2/15)T^4$  is the energy density for photon gas<sup>5</sup>. Let us note that Helium abundance depends upon two parameters,  $T_f$  and  $\eta$ , which can be used to constrain  $\Delta N_\nu$ . The constraint can be improved considerably by considering, in addition, the Deuterium

abundance and CMB data [151]. However, in this case, we should estimate the ratio (45) below the  $e^+e^-$  annihilation temperature,  $T_{e^+e^-}$ . After electron positron annihilation,  $T_\nu = (4/11)^{4/3}T$  such that

$$\left(\frac{\rho_X}{\rho_\gamma}\right)_{T_{e^+e^-}} \leq \frac{7}{8} \left(\frac{4}{11}\right)^{4/3} \Delta N_\nu \quad (46)$$

An observational constraint on  $\Delta N_\nu$  should put a restriction on the extra degree of freedom that is not part of the standard model. Remember that, in scalar field models with tracking behaviour,  $\rho_\phi \propto a^4$  during the radiation era, and the fraction of total energy that  $\rho_\phi$  comprises is determined by the slope of the steep exponential potential responsible for scaling behaviour. Using combined data gives  $N_\nu < 3.2$  at a 95% confidence level, which implies a bound on the slope of the potential [150],

$$\left(\frac{\rho_X}{\rho_\gamma}\right)_{T_{e^+e^-}} \simeq \Omega_\phi|_{T_{e^+e^-}} = \frac{4}{\alpha^2} \lesssim \frac{7}{8} \left(\frac{4}{11}\right)^{4/3} \times 0.2 \Rightarrow \alpha \gtrsim 10. \quad (47)$$

It may be noted that in the case of thawing models,  $\Omega_\phi \ll 1$  and the BBN constraint is trivially satisfied. Similarly, for relic gravity waves,  $\rho_{GW}$  should satisfy the following bound:

$$\left(\frac{\rho_{GW}}{\rho_\gamma}\right)_{T_{e^+e^-}} \leq \frac{7}{8} \left(\frac{4}{11}\right)^{4/3} \Delta N_\nu \quad (48)$$

which can be translated into a bound on  $\Omega_{GW,0}$ ,

$$\Omega_{GW,0} = \frac{7}{8} \left(\frac{4}{11}\right)^{4/3} \Omega_{\gamma,0} \Delta N_\nu \simeq 5.6 \times 10^{-6} \Delta N_\nu \quad (49)$$

where we used the fact that  $\rho_{GW} \sim \rho_\gamma \sim a^{-4}$  and also used the observed value of the fractional energy density of radiation at the present epoch,  $\Omega_{\gamma,0} \simeq 2.47 \times 10^{-5}$ . Using the combined abundances of Helium and Deuterium with the CMB data ( $\Delta N_\nu \lesssim 0.2$ ), we finally have

$$\Omega_{GW,0} \lesssim 1.12 \times 10^{-6} \quad (50)$$

which puts an upper bound on the kinetic regime or the lower bound on the reheating temperature in models of quintessential inflation; see Section 5 for details.

### 3.5. Dynamics with General Class of Potentials and Emergence of Scaling Behaviour in the Asymptotic Regime

As discussed in the preceding sub-section, scaling solutions are specific to exponential potential, which are either suited to field-dominated situations or scaling behaviour but not to both simultaneously. Thus, we might use a potential suitable for inflation that subsequently changes to an exponential form soon after inflation ends, or think of a non-exponential type of potential capable of addressing the inflationary requirements at an early time and dynamically mimicking the exponential behaviour in the post-inflationary era.

Exponential potential has a distinguishing feature: its slope,  $\lambda_s \equiv -M_{Pl} V_\phi / V$ , is constant. In this case, we have two dynamical variables,  $x$  and  $y$ , and correspondingly two autonomous equations. For a potential that is not an exponential, the slope becomes a variable quantity and one needs an additional dynamical equation for  $\lambda_s$  [136,152–154]:

$$x' = f(x, y, \lambda_s); \quad y' = g(x, y, \lambda_s) \quad (51)$$

$$\lambda_s' = -\sqrt{6} \lambda_s^2 (\Gamma - 1) x \quad (52)$$

$$\Gamma = \frac{V_{\phi\phi} V}{V_\phi^2} \quad (53)$$

where  $\Gamma$  is an important field construct that controls the dynamics of the system with a general type of potential. For the exponential function,  $\Gamma = 1$ , corresponding to a constant slope of the potential, making Equation (52) redundant. In this case,  $\rho_\phi$  scales as background energy density  $\rho_b$ , giving rise to a scaling solution that is an attractor of dynamics. Without loss of generality, we may consider a class of potentials in which field  $\phi$  rolls down the potential from smaller to larger values ( $\phi \rightarrow \infty$ ) such that  $x > 0$ .

In the case of potentials with  $\Gamma > 1$ , for instance,

$$V = V_0 \frac{M_{Pl}^n}{\phi^n}; \quad \Gamma = 1 + 1/n \quad (n > 1), \quad (54)$$

the slope decreases with evolution—see Equation (52)—eventually giving rise to slow roll and forcing the field to evolve to quasi de Sitter ( $\rho_\phi \simeq \text{const.}$ ,  $w_\phi \simeq -1$ ), which is an attractor [153]. While the field is rolling down the steep part of the potential ( $\lambda_s$  is large),  $\rho_\phi$  closely follows the background [122],

$$w_\phi = \frac{2\Gamma}{2\Gamma - 1} = w_b + \frac{2}{n}(1 - w_b) \quad (55)$$

It should be noted that for generic values of  $n$ ,  $w_\phi \simeq w_b$  and  $\Gamma \simeq 1^6$ . However, in this case, ( $\Gamma > 1$ ), and the slope ( $\lambda_s = n/\phi$ ) decreases with evolution such that the field enters the slow roll regime at late stages,

$$w_\phi = -1 + \frac{\lambda_s^2}{3} \rightarrow -1, \quad \lambda_s \rightarrow 0 \quad (56)$$

and can account for late time acceleration. A scalar field solution that mimics the background in the post-inflationary era and only at late stages overtakes it to account for the observed late time acceleration has been termed a *tracker*; see Figure 2a. Obviously, the class of potentials with  $\Gamma > 1$  are of interest and have been widely investigated in the literature.

On the other hand, if  $\Gamma < 1$ , the slope of the potential increases with evolution such that the field runs down its potential faster and faster, making the potential energy redundant, and naturally ends up in the kinetic regime with  $\rho_\phi \sim a^{-6}$ . In this case, it follows from (53) that the slope increases,

$$\frac{1}{\lambda_s} = \int x(\Gamma - 1)dN \quad (57)$$

and in the process of evolution, as  $\lambda_s$  becomes large and  $\Gamma \rightarrow 1$ . In this case, the system would eventually join the scaling track in the asymptotic regime. We shall demonstrate this in an example. On the other hand, during evolution,  $\lambda_s \rightarrow 0$  if we begin from  $\Gamma > 1$  ( $\Gamma \neq \text{Constant}$ ), and in this case,  $\Gamma$  increases towards infinity. In a sense, “ $\Gamma$ ” defines the type of steepness of the potential: *the slope tells us about the steepness of the potential, whereas  $\Gamma$  expresses whether, with evolution, the steepness is unchanged ( $\Gamma = 1$ ), increases ( $\Gamma < 1$ ) or decreases ( $\Gamma > 1$ )*. Potentials with  $\Gamma < 1$  ( $\Gamma > 1$ ) are sometimes referred to in the literature as steeper (shallower) than the exponential potential for brevity. It is interesting to think of slope  $\lambda_s(\phi)$  as defined over the smooth set of functions  $\{V(\phi)\}$ . Since

$$\frac{d\lambda_s}{d\phi} = -\lambda_s^2(\Gamma - 1) = 0 \rightarrow \Gamma = 1, \quad (58)$$

slope,  $\lambda_s$ , is the extremum for an exponential function. The second derivative,

$$\frac{d^2\lambda_s}{d\phi^2} = -\frac{1}{V_\phi^4} \left( V_\phi^2 (V_{\phi\phi\phi} V + V_{\phi\phi} V_\phi) - 2V_{\phi\phi}^2 V_\phi V \right) \quad (59)$$

computed for exponential potentials, also vanishes. Thus,  $\Gamma = 1$  is the saddle point in the functional space, which explains the mentioned features of the dynamics.

It is desirable that, for most of the history of the Universe, the field follows the background (scaling behaviour), and only at late stages does it exit the scaling regime, taking over the background to become the dominant component, and might mimic dark energy. In what follows, we discuss how to incorporate this feature into the dynamics.

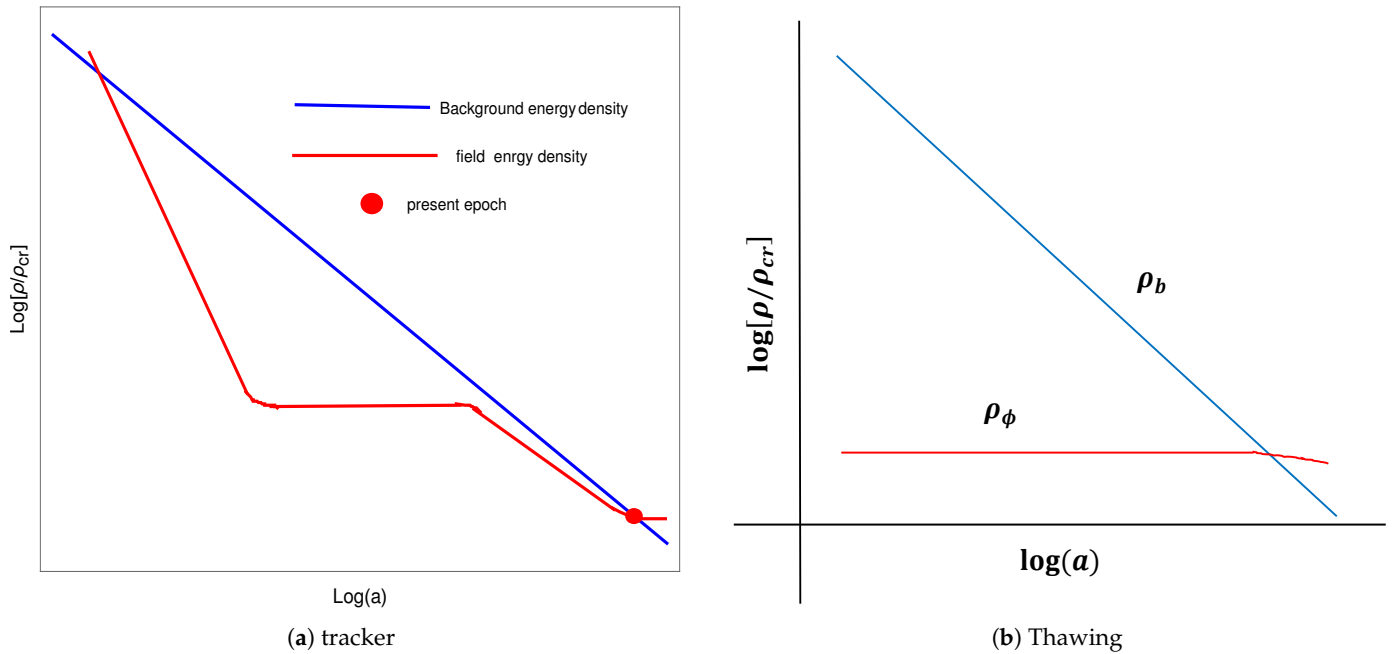


**Figure 2.** (a) shows evolution of field energy density  $\rho_\phi$  and background matter density (radiation/cold matter) versus  $\ln(a)$  for a potential shallower than the exponential potential ( $\Gamma > 1$ )—for instance, inverse power law potentials,  $V \sim \phi^{-n}$ ,  $n > 0$  with  $\Gamma = 1 + 1/n$ . After recovery from the freezing regime, the field on the steep part of the potential evolves with an equation of state parameter close to that of the background. In this case, the slope of the potential gradually decreases and the scalar field slowly moves towards the background and overtakes it and joins the slow roll with a diminishing value of the slope *à la a tracker*. (b) shows schematic representation of thawing quintessence, where the field is frozen on a flat potential due to Hubble damping. When  $\rho_\phi$  approaches the background energy density at late times, the field resumes slow roll and accounts for late time acceleration.

Making a Perfect Tracker from Scaling Solutions:  $\Gamma = 1$  and  $\Gamma < 1$

In view of the above, one needs a steep exponential type of behaviour in the post-inflationary era with a mechanism of late time exit to acceleration *à la a tracker* not sensitive to initial conditions. In the framework of quintessential inflation, one could design a potential that changes to shallow exponential, is suitable for inflation at early epochs and reduces to a steep exponential function in the post-inflationary era. It is easier to accomplish this task using non-canonical scalar field action [130,155],

$$\mathcal{S} = \int d^4x \sqrt{-g} \left[ \frac{M_{Pl}^2}{2} R - k^2(\phi) \partial_\mu \phi \partial^\mu \phi - V(\phi) \right] \quad (60)$$

$$k^2(\phi) = \left( \frac{\alpha^2 - \tilde{\alpha}^2}{\tilde{\alpha}^2} \right) \frac{1}{1 + \beta^2 e^{\alpha\phi/M_{Pl}}} + 1 \quad (61)$$

$$V = M_{Pl}^4 e^{-\alpha\phi/M_{Pl}} \quad (62)$$

where,  $\alpha$ ,  $\tilde{\alpha}$  and  $\beta$  are constants to be chosen by the requirement of model building. Let us use the following transformation

$$\sigma = f(\phi) \quad (63)$$

$$k^2 = \frac{\partial f}{\partial \phi} \quad (64)$$

to change the action to canonical form:

$$S = \int d^4x \sqrt{-g} \left[ \frac{M_{Pl}^2}{2} R - \partial_\mu \sigma \partial^\mu \sigma - V(f^{-1}(\sigma)) \right] \quad (65)$$

The effect of canonicalisation is pushed into the potential, which we need to work out in the small and large field limits to demonstrate the viability of the underlying construction to early and late time dynamics. To this effect, we need to express the canonical field  $\sigma$  through field  $\phi$  for  $\tilde{\alpha} < 1$  and  $\alpha \gg \tilde{\alpha}$ . In the small field limit, where we expect inflation, we have<sup>7</sup>

$$\phi \ll -2M_{Pl} \ln \beta/\alpha \Rightarrow k^2(\phi) \simeq \frac{\alpha^2}{\tilde{\alpha}} \quad (66)$$

$$\sigma(\phi) \simeq \frac{\alpha}{\tilde{\alpha}} \phi \Rightarrow V \propto e^{-\tilde{\alpha}\sigma/M_{Pl}} \quad (67)$$

which can give rise to inflation for  $\tilde{\alpha} < 1$ . In the large field approximation,

$$\phi \gg -2M_{Pl} \ln \beta/\alpha \rightarrow k^2(\phi) \simeq 1 \Rightarrow V \propto e^{-\alpha\sigma/M_{Pl}}, \quad (68)$$

with a desired scaling behaviour in the post-inflationary era. It is therefore not surprising that the Lagrangian (62) can successfully describe inflation at early times and with scaling behaviour in the post-inflationary era.

In the canonical formulation, an interesting possibility is provided by a class of non-exponential types of potentials that are flat initially, followed by steep behaviour that is exponential, as in the asymptotic regime,  $\Gamma \rightarrow 1$  for large values of the field. To this effect, it is interesting to examine a class of generalised exponential potentials [130],

$$V(\phi) = V_0 e^{-\alpha\phi^n/M_{Pl}^n}; \quad n > 1 \quad (69)$$

which can support slow roll ( $\lambda_s = \alpha\phi^{n-1}$ ) at early times when  $\phi$  is small, followed by a steep behaviour after inflation ends. In this case, slope ( $\lambda_s(\phi)$ ) is a dynamical variable whose evolution is dictated by  $\Gamma$ ,

$$\Gamma(\phi) = 1 - \frac{n-1}{n\alpha} \left( \frac{M_{Pl}}{\phi} \right)^n \quad (70)$$

which approaches one from below for large values of  $\phi/M_{Pl}$ . Before the asymptotic region is reached,  $\Gamma < 1$  and (69) exhibits the properties of a function steeper than the exponential potential, pushing the field into the kinetic regime. However, for large values of the field, (69) dynamically mimics the behaviour of an exponential potential ( $\Gamma \rightarrow 1, \phi \rightarrow \infty$ ), allowing the field to finally catch up with the background. Does the field continue in the kinetic regime when  $\Gamma < 1$ ? In what follows, we describe a phenomenon that occurs when the field  $\phi$  runs down a steep potential in the presence of background matter density. Thereafter, we shall be able to narrate the complete story of field dynamics in a steep potential.

### 3.6. Slow Roll in Presence of Background Matter: Freezing Regime

The formalism of slow roll parameters can be applied to quintessence, keeping in mind that the Hubble rate is not solely defined by the scalar field energy density: background matter density also contributes to it.

It should be noted that, unlike in the case of inflation, slow roll parameters might be useful here only for a broad perspective. An interesting feature of field dynamics is noticed for a field rolling down a steep potential when its energy density is negligible compared

to the background energy density. In this case, the field freezes on its potential and waits there for a conducive situation to resume motion. Indeed, in the case of slow roll<sup>8</sup>

$$\dot{\phi}^2/2 \ll V \implies \epsilon = 3 \frac{\dot{\phi}^2/2}{\rho_\phi} \simeq \frac{3}{2} \frac{\dot{\phi}^2}{V} = \frac{1}{6} \frac{V_\phi^2}{VH^2}, \quad (71)$$

where we used the slow roll value of  $\dot{\phi}$ . In what follows, we are interested in the case when  $\rho_\phi \ll \rho_b$  such that  $H^2 \simeq \rho_b/3M_{Pl}^2$ ,

$$\epsilon = \frac{M_{Pl}^2}{2} \left( \frac{V_\phi}{V} \right)^2 \left( \frac{\rho_\phi}{\rho_b} \right) \equiv \epsilon_0 \left( \frac{\rho_\phi}{\rho_b} \right) \quad (72)$$

$$\epsilon = \frac{\lambda_s^2}{2} \left( \frac{\rho_\phi}{\rho_b} \right) \quad (73)$$

Since we are dealing with a steep potential,  $\epsilon_0 > 1$ , but interestingly,  $\epsilon \ll 1$  as  $\rho_b \gg V(\phi)$ —*Hubble damping*. Thus, unlike the case of inflation, slow roll becomes operative here due to Hubble damping. However, this is not useful for dark energy as  $\rho_\phi \ll \rho_b$  in this case, but it is certainly useful for the understanding of scalar field evolution in a steep potential<sup>9</sup>. As a result of Hubble damping, the field is frozen on its potential and waits there till the ratio  $\rho_\phi/\rho_b$  acquires a specific numerical value ( $\rho_b \sim a^{-3(1+w_B)}$ ,  $\rho_\phi = Const$ ) given by Equation (73) when slow roll is violated ( $\epsilon = 1$ ). Field evolution then commences but, hereafter, the field dynamics crucially depends upon the type of steepness of the potential. We shall come back to this point in the sub-section on post-inflationary evolution.

### 3.6.1. Recovery from Freezing Regime

For the sake of illustration, let us focus on a steep exponential potential. After recovering from the freezing regime, which happens due to slow roll violation, the scalar field joins the scaling track. However, when this happens, it crucially depends upon the numerical value of the slope of the potential. Indeed, slow roll (72) is violated when

$$\epsilon \simeq 1 \implies \left( \frac{\rho_\phi}{\rho_b} \right) \simeq \frac{2}{\alpha^2}; \quad \lambda_s^2 = \alpha^2 > 3, \quad (74)$$

which tells us that the larger is the numerical value of  $\alpha$ , the smaller is the ratio  $\rho_\phi/\rho_b$ , when the field resumes evolution. Actually, when slow roll ends, the scalar field begins running down the steep potential, its kinetic energy gradually increases to the scaling value<sup>10</sup> and it joins the scaling regime, it has no other option as the scaling solution is an attractor in this case. Hence, as the field recovers from freezing and resumes evolution, it always finds itself on the entry to the scaling regime, irrespective of the numerical value of the ratio  $\rho_\phi/\rho_b$ . As a result, even if the field energy density constitutes a negligible fraction of the total energy, the scalar field joins the scaling track. In fact, this phenomenon has a simple physical meaning: a particle can move in a medium despite large friction if the force acting on it (gradient of the force field potential) is large. This remark about the interplay between the slope of the potential and the ratio of the field to background matter energy densities is especially important in relation to asymptotic scaling solutions, which we will shortly discuss.

### 3.6.2. Slowly Rolling Quintessence

Though slow roll parameters do not play a similar role for quintessence, they are still helpful for a general perspective. The slow roll conditions should be used with caution here because, unlike inflation, the Hubble parameter receives a contribution from background matter in this case. Quintessence models can be classified as thawing models [156,157] (see also [158,159]) and tracker models [122,160]. In the first category, the scalar field is initially frozen on a shallow potential due to the Hubble damping. The field recovers from the freezing regime ( $w_\phi = -1$ ) at late stages and rolls slowly along a shallow potential, increasing

the equation of state parameter to a level consistent with observation; see Figure 2b. As for the trackers, after recovery from the freezing regime, the field (approximately) follows the background and only at late times does it quit to join the slow roll due to the shallow nature of the potential around the present epoch; see Figure 2a. For thawing models,  $1/2 < \beta < 3/2$  and the friction term is not operative here, whereas the friction term is large,  $\beta \ll 1$ , in the case of trackers [156]. We shall assume that  $\beta$  does not change much during slow roll in the thawing case. In terms of  $\beta$ , scalar field Equation (8) can be cast as (see [161] for details)

$$\dot{\phi} = -\frac{V_{\phi}}{3(1+\beta)H} \quad (75)$$

We then ask for the consistency of  $\beta$  being  $\mathcal{O}(1)$  (thawing models) or  $\beta \simeq 0$  (trackers) with the field Equation (8). Indeed, differentiating Equation (75) with respect to time, we have

$$-\frac{\beta V_{\phi}}{1+\beta} = \ddot{\phi} \simeq -\frac{(1+w_b)}{2(1+\beta)} + \frac{V_{\phi\phi}V_{\phi}}{9(1+\beta)^2H^2} \Rightarrow \beta \simeq \frac{(1+w_b)}{2} - \frac{V_{\phi\phi}}{9(1+\beta)H^2} \quad (76)$$

where we have ignored the term  $\dot{\beta}/\beta H$  and used  $-\dot{H}/H^2 \simeq 3(1+w_b)/2$ . In the thawing case,  $\beta$  is assumed to be approximately constant, and since the second term on the right-hand side of (76) is time-dependent, it is necessary for the equality to hold that

$$|\eta| \ll 1 \Rightarrow \beta = \frac{3}{2}(1+w_b) \quad (77)$$

where we used the fact that  $\beta = \mathcal{O}(1)$ . We find that our assumption that  $\beta$  is constant is consistent with the field equation. On the other hand,  $|\beta| \ll 1$  for trackers and we find the consistency condition

$$\eta = \frac{3}{2}(1+w_b) \quad (78)$$

which gives an order of magnitude estimate for the mass of quintessence, namely  $m \simeq H_0 \sim 10^{-33}$  eV.

### 3.6.3. The Asymptotic Scaling Solution

We argued that the class of potentials with  $\Gamma < 1$  mimic scaling behaviour in the asymptotic regime. The generalised exponential potential (69), shallow initially ( $\phi/M_{Pl} \ll 1$ ) with asymptotic features of an exponential potential in the post-inflationary region, is a suitable candidate for quintessential inflation. As  $\Gamma \rightarrow 1$  for large values of  $\phi/M_{Pl}$ , we expect a scaling regime in the asymptotic region. We need to set an autonomous system with a suitable choice of variables; the choice for  $X$  &  $Y$  is obvious, and the third variable should explicitly include information about the asymptotic nature of the scaling solution [146],

$$X \equiv \frac{\phi^2}{2V}; \quad Y \equiv \frac{V_{\phi}}{\dot{\phi}H} \quad (79)$$

$$A \equiv \frac{1}{\phi/M_{Pl} + 1} \quad (80)$$

Let us cast the equation of motion in autonomous form in the case of potential (69) using variables defined in (80) and (79),

$$\begin{aligned} \frac{dx}{dN} &= -2X(3+Y+XY) \\ \frac{dY}{dN} &= 2XY^2 \left( 1 - \frac{(n-1)A^n}{\alpha n(1-A)^n} \right) + Y(9/2 + Y + 3w_b/2) - \end{aligned} \quad (81)$$

$$XY^3 A^{2n-2} (X(w_b - 1) + w_b + 1) \left[ \frac{A - 1}{\alpha n (1 - A)^n} \right]^2 \quad (82)$$

$$\frac{dA}{dN} = \frac{2XYA^{n+1}(1-A)}{\alpha n(1-A)^n} \quad (83)$$

Let us also express other quantities of interest through autonomous variables:

$$\Gamma = 1 - \frac{(n-1)A^n}{\alpha n(1-A)^n} \quad (84)$$

$$w_\phi = \frac{X-1}{X+1} \quad (85)$$

$$w_\phi = \frac{2}{3}(X+1)XY^2 A^{2n-2} \frac{1}{\alpha^2 n^2 (1-A)^{2n-2}} \quad (86)$$

Since  $\Gamma = 1$  for  $A = 0$  ( $\phi \rightarrow \infty$ ), the system should mimic the properties of exponential potential; thereby, we expect scaling behaviour in the asymptotic regime. Indeed, we find the critical point,

$$X = \frac{1+w_b}{1-w_b}; \quad Y = \frac{3}{2}(w_b-1); \quad A = 0 \quad (87)$$

as expected. It was demonstrated in reference [146] that the asymptotic scaling solution (87) is an attractor. It should be noted that in the case of  $n = 1$ , the third Equation (83) decouples from the other two equations, which can be solved without reference to (83), which encodes the information about the asymptotic condition, and we recover a standard result corresponding to exponential potential. It is important to note that unlike the case of exponential potential, here, we cannot infer the time dependence of physical quantities in the scaling regime by the critical values in (87) as the fixed point is reached in the limit,  $t \rightarrow \infty$ ;  $\phi \rightarrow \infty$ . Substituting the critical point in the expressions for  $\Gamma$ ,  $w_\phi$  &  $\Omega_\phi$ , we have

$$\text{Asymptotic scaling solution : } \Gamma \rightarrow 1; \quad w_\phi \rightarrow w_m; \quad \Omega_\phi \rightarrow 0 \quad (88)$$

In this case, passage to the fixed point can be studied numerically. To analytically understand the field dynamics, we need an ansatz in the asymptotic regime whose consistency with the field equation should be checked. We have the following ansatz in the asymptotic regime ( $t \rightarrow \infty$ ) [162] (see [163] for comparison)

$$\alpha \left( \frac{\phi(t)}{M_{Pl}} \right)^n = f_0 \ln \left( \frac{t}{t_1} \right) + f_1 \ln \left[ \ln \left( \frac{t}{t_1} \right) \right] + \dots \quad (89)$$

Substituting (89) in the field Equation (8) and keeping in mind the asymptotic behaviour, we find

$$f_0 = 2; \quad f_1 = \frac{2(n-1)}{2}; \quad t_1^2 = \frac{M_{Pl}^2(1-w_b)}{V_0 n^2 (1+w_b) \alpha^{2/n} 2^{(n-1)/n}}, \quad (90)$$

which allows us to compute important parameters in the asymptotic regime showing passage to the critical point (87),

$$w_\phi = w_b + (w_b^2 - 1) \frac{(n-1)^2 \ln \left[ \ln \left( \frac{t}{t_1} \right) \right]}{n^2 \ln \left( \frac{t}{t_1} \right)} \rightarrow w_b, \quad t \rightarrow \infty \quad (91)$$

$$\Omega_\phi = \frac{3(1+w_b)}{4n^2} \left( \frac{2}{\alpha} \right)^{2/n} \left[ \ln \left( \frac{t}{t_1} \right) \right]^{2(1-n)/n} \rightarrow 0, \quad t \rightarrow \infty \quad (n > 1) \quad (92)$$

which obviously reduce to the standard results for  $n = 1$ . We have, therefore, demonstrated that the scalar field system in the case of the generalised exponential potential (69) with

$\Gamma < 1$  eventually comes to the scaling track in the asymptotic regime. We also analytically demonstrate the passage to the critical point. We had argued that a scalar field with an arbitrary steep potential with  $\Gamma < 1$  should ultimately join the scaling track. In view of quintessential inflation, it is desirable that  $\Gamma \simeq 1$  for quite some time while  $\phi$  is rolling on the steep part of the potential<sup>11</sup> and  $\rho_\phi$  follows the background energy density before exiting to acceleration to mimic tracker-like behaviour. Depending upon the underlying field potential, an approximate scaling regime might be invisible if the overshoot of background energy density is so deep that the field freezes on its shallow part and, after recovery from Hubble damping, it enters the slow roll mimicking dark energy—*thawing realisation*; see Figure 3. Obviously, no exit mechanism is required in this model but late time physics is sensitive to initial conditions. Let us once again reiterate that, in the case of the generalised exponential potential (69), with an exit mechanism, we have the desired situation to realise a perfect tracker.

Using the above given technical information on scalar field dynamics, we would be in a position to describe the scalar field dynamics in the presence of background in the post-inflationary era. This would give us the appropriate perspective of the unification of inflation with late time acceleration without interfering with the thermal history of the Universe, and good accuracy can be achieved.

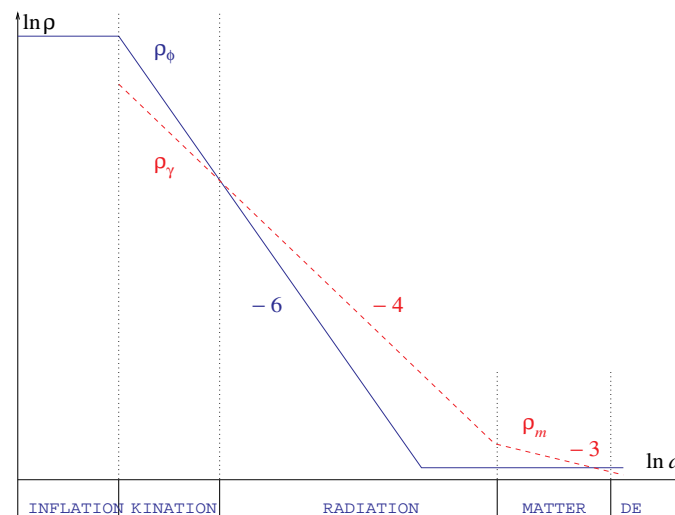


**Figure 3.** Qualitative behaviour of  $\rho_\phi$  for the potential used in Ref. [63] ( $V \sim \exp[1 - \tanh(\phi)] - 1$ ), which is shallow initially and at late stages and steep in between. In this case, overshoot is deep enough that the field freezes at the shallow part of the potential. After recovering from Hubble damping, it rolls slowly and adheres to late time acceleration (figure is adapted from Ref. [63]).

#### 4. Post-Inflationary Dynamics: The Exit Mechanism via Coupling with Massive Neutrino

In the preceding sub-sections, we described scalar field dynamics with and without the presence of background energy density  $\rho_b$ . We argued that the runaway potential generic to the underlying framework should be steep in the post-inflationary era. The energy density of radiation produced at the end of inflation  $\rho_r^{end}$  in this framework is typically several orders of magnitude lower than  $\rho_\phi^{end}$ , and the radiative regime takes a long time to begin. After inflation ends, the field rolls down the steep potential rapidly, making the potential energy redundant. As a result, the field evolves in the kinetic regime ( $\rho_\phi \sim a^{-6}$ ) and eventually undershoots the background such that  $\rho_\phi \ll \rho_b$ . When this happens, the field enters the slow roll due to Hubble damping and freezes ( $\rho_\phi = const$ ) on its potential (see Equation (72) and waits there till the background energy density ( $\rho_b \sim a^{-m}$ ;  $m = 4, 3$  for radiation and matter, respectively) becomes comparable to  $\lambda_s^2 \rho_\phi / 2$ ; slow roll is then violated and the evolution of the field resumes. Hereafter, the field dynamics crucially depends upon the nature of the steepness of the potential, which is dictated by  $\Gamma$ . For exponential potential  $\Gamma = 1$ , the scalar field would follow the background as the scaling

solution is an attractor in this case; see Figure 4a. If  $\Gamma < 1$ , the slope of the potential increases, giving rise to the increase in kinetic energy; the field energy density would then move away from the background and evolve in the kinetic regime, ending up in the freezing regime when  $\rho_\phi \ll \rho_b$  and so on and so forth. However, the slope always increases during evolution, and when it reaches large values,  $\Gamma$  then approaches its scaling value,  $\Gamma = 1$ ; see Equation (57). As a result, the system eventually joins the scaling track; see Figure 4b. In the case of generalised exponential potential (69), we demonstrated that the scaling solution is an attractor in the asymptotic regime. In this case,  $\lambda_s \sim (\ln(t))^{(1-1/n)}$ ,  $\Omega_\phi \rightarrow 0$  and  $w_\phi \rightarrow w_b$  for  $t \rightarrow \infty$ . Obviously, in this case, there is no issue related to nucleosynthesis. It should be noted that the nucleosynthesis constraint imposes a lower bound on  $\alpha$  for exponential potentials corresponding to a small fraction of field energy density, which is automatically true for asymptotic scaling solutions as  $\Omega_\phi \rightarrow 0$  in this case.

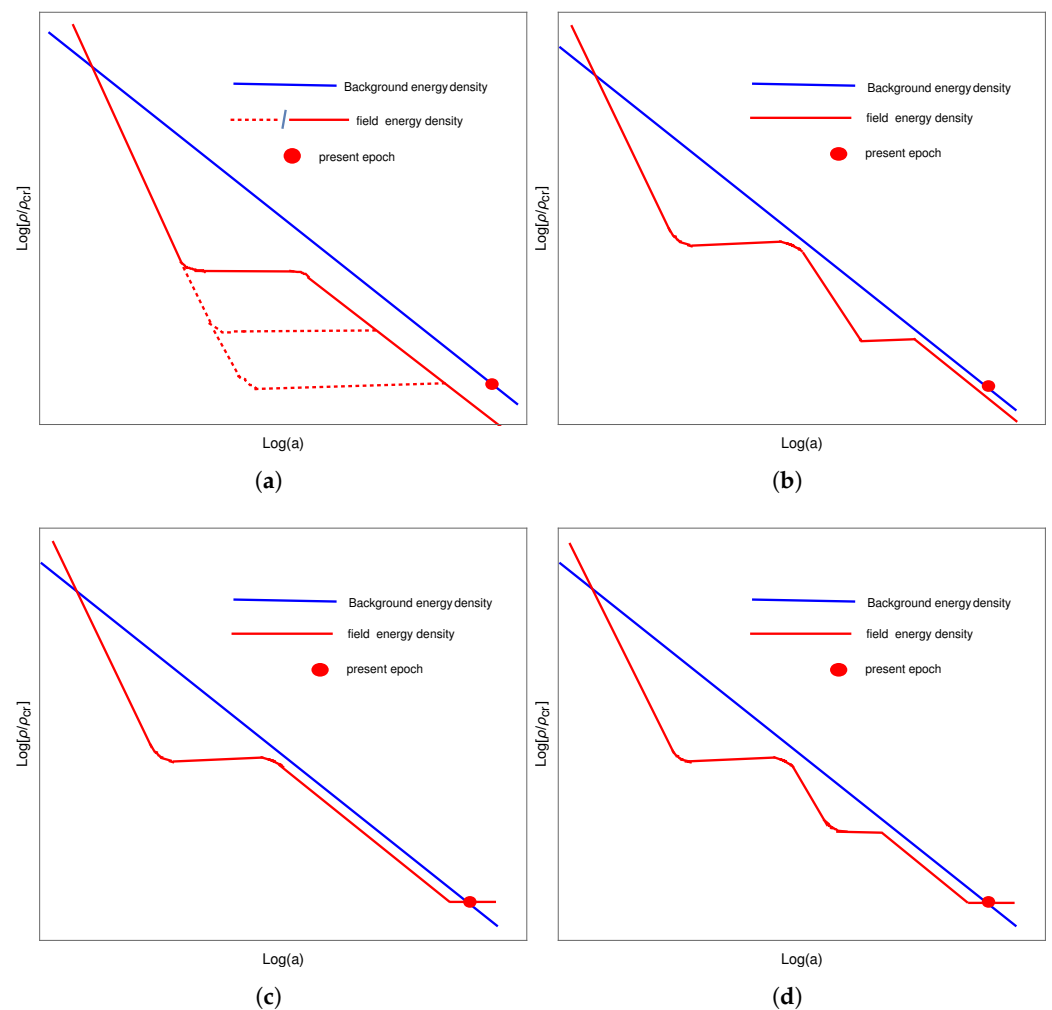


**Figure 4.** Figure shows the qualitative behaviour of  $\rho_\phi$  along with the energy density of background matter (cold matter/radiation) versus  $\ln a$  for a steep potential. As  $\rho_\phi$  overshoots the background energy density ( $\rho_\phi \ll \rho_b$ ,  $\rho_b$  designates background matter energy density), the field freezes on its potential due to Hubble damping. After the recovery from freezing, field evolution crucially depends upon the nature of the steepness of the potential. (a) In case of the exponential potential ( $\Gamma = 1$ ), the field catches up with the background and tracks it forever. (b) exhibits the general feature of scalar field dynamics for a field potential steeper than the exponential potential ( $\Gamma < 1$ ): after recovery from freezing,  $\rho_\phi$  evolves in steps (down and right) and eventually catches up with the background [130]—asymptotic scaling solution. (c,d) show exit from scaling and asymptotic scaling regimes to late time acceleration at the present epoch *à la* a *perfect tracker*. Exit is triggered due a late time feature in the runaway potential that makes it shallow at late stages of evolution.

If  $\Gamma > 1$  (inverse power law potentials), the slope of the potential  $\lambda_s$  decreases when the field rolls along the steep part of the potential with a large value of  $\lambda_s$ ; it evolves with an equation state  $w_\phi$ , which is close to the equation of state of background matter for generic values of  $n$ —*approximate scaling behaviour*. However,  $\lambda_s$  decreases with evolution, causing the field energy density to gradually move towards the background and eventually overtake it at late times; the field then enters a slow roll with a diminishing slope ( $w_\phi \rightarrow -1$ ) that accounts for late time acceleration; see Figure 2a. Setting the model parameters appropriately, one makes the framework consistent with observation. The change in initial conditions related to scalar field dynamics, within a broad range, changes the time for field entry into the (approximate) scaling regime, leaving the late time physics unchanged. A remark about “generic” initial conditions is in order. One can choose extraordinary field initial conditions, giving rise to a deep overshoot, allowing the field to recover from Hubble damping only at late times in the region of slow roll, such that the observational consistency is guaranteed. Late time physics, in this case, would become sensitive to initial conditions, necessitating a readjustment of the model parameters to ensure observational consistency—*thawing realisation*.

In the case of the generalised exponential potential, an interesting dynamical feature is observed, where  $\rho_\phi$  initially evolves in steps (down and forward) and eventually catches up with the background in the asymptotic region as  $\Gamma \rightarrow 1$ . Let us once again reiterate that the scaling, or at least asymptotic scaling behaviour in the post-inflationary era, is required for viable cosmological dynamics. Secondly, since the scaling solution is an attractor, which is non-accelerating, one needs a late time feature in the potential to mimic slow roll, allowing the exit to late time acceleration, dubbed a perfect tracker; see Figure 4c,d.

In what follows, we shall analyze an exit mechanism based upon scalar field coupling to massive neutrino matter, which modifies the scalar field potential. The coupling is effective only at late stages of evolution, where the effective potential has a minimum, allowing the field to settle there at a late times, and an exit to a quasi de Sitter phase is realised.

The late time exit for steep runaway potential can be realised by non-minimal coupling of the quintessence field to matter, which modifies the runaway potential such that the effective potential has a minimum (see Refs. [124,164,165] for other kinds of exit mechanism). The conformal coupling of field to matter under consideration is proportional to the trace of energy momentum tensor of matter and vanishes identically during radiation. Coupling becomes operative after matter domination is established, giving rise to an effective potential that has a minimum, which is the right feature at the wrong time. In general, minimum in the potential where the field can settle down leads to de Sitter-like behaviour and is unwanted in this case, as it can spoil the matter phase; it is more than desirable to leave the matter phase intact. The problem finds its solution in the coupling to massive neutrino matter, which acquires a non-vanishing value only at late times when massive neutrinos become non-relativistic [130,155,166,167].

Let us consider the action that describes coupling between massive neutrino matter and the scalar field [127,168],

$$\mathcal{S} = \int d^4x \sqrt{-g} \left[ \frac{M_{\text{Pl}}^2}{2} R - \frac{1}{2} \partial_\mu \phi \partial^\mu \phi - V(\phi) \right] + \mathcal{S}_m + \mathcal{S}_r + \mathcal{S}_\nu \left( A^2(\phi) g_{\alpha\beta}, \Psi_\nu \right), \quad (93)$$

where  $\mathcal{S}_m$ ,  $\mathcal{S}_r$  and  $\mathcal{S}_\nu$  are actions for cold matter, radiation and neutrino matter, respectively.  $g_{\mu\nu}$  and  $\tilde{g}_{\mu\nu} \equiv A^2(\phi) g_{\mu\nu}$  designate the Einstein and Jordan metrics. It is important to note here that the metric for the neutrino action is different from the rest (including matter and gravity part). One should, therefore, be careful while deriving the relevant quantities from this action. In this section, we shall explicitly derive the continuity equation using (93) for neutrino matter and the scalar field in the Einstein frame. Let us note that, in the Jordan frame, neutrino matter is minimally coupled and its energy momentum tensor obeys the

standard conservation law. In the Jordan frame, the energy momentum tensor for neutrino matter is given by

$$\tilde{T}_{\mu\nu} = \frac{-2}{\sqrt{-\tilde{g}}} \frac{\delta \mathcal{S}}{\delta \tilde{g}^{\mu\nu}} = \begin{pmatrix} \tilde{\rho} & 0 & 0 & 0 \\ 0 & & & \\ .0 & & \tilde{a}^2 \tilde{p} & \\ 0 & & & \end{pmatrix} \quad (94)$$

or equivalently

$$\tilde{T}^{\mu}{}_{\nu} = \text{diag}(-\tilde{\alpha}, \tilde{p}, \tilde{p}, \tilde{p}), \quad (95)$$

which satisfies the standard continuity equation,

$$\tilde{\nabla}_{\mu} \tilde{T}^{\mu\nu} = 0 \quad (96)$$

$$\dot{\tilde{\rho}} + 3\tilde{H}(\tilde{\rho} + \tilde{p}) = 0. \quad (97)$$

Since the Einstein and Jordan metrics are related via the conformal factor  $A^2(\phi)$ , we have the following relations:

$$\begin{aligned} g_{\mu\nu} &= A^{-2} \tilde{g}_{\mu\nu} \\ g^{\mu\nu} &= A^2 \tilde{g}^{\mu\nu} \\ \sqrt{-g} &= A^{-4} \sqrt{\tilde{g}} \\ a &= A^{-1} \tilde{a} \\ dt &= A^{-1} \tilde{d}t. \end{aligned} \quad (98)$$

Let us note that the energy momentum tensor in the Einstein frame with metric  $g_{\mu\nu}$  is related to its counterpart in the Jordan frame,

$$T_{\mu\nu} = \frac{-2}{\sqrt{-g}} \frac{\delta \mathcal{S}}{\delta g^{\mu\nu}} = \frac{-2}{A^{-4} \sqrt{\tilde{g}}} \frac{\delta \mathcal{S}_{\nu}}{\delta \tilde{g}^{\mu\nu}} = A^2 \tilde{T}_{\mu\nu}. \quad (99)$$

We can compare the individual components of stress–energy tensors of the two frames by the following manipulation:

$$T^{\mu}{}_{\nu} = g^{\mu\alpha} T_{\alpha\nu} = A^2 \tilde{g}^{\mu\alpha} A^2 \tilde{T}_{\alpha\nu} = A^4 \tilde{T}^{\mu}{}_{\nu} \Rightarrow \tilde{\rho} = A^{-4} \rho, \quad \tilde{p} = A^{-4} p. \quad (100)$$

The Hubble parameters for the two frames are related as

$$H = \frac{1}{a} \frac{da}{dt} = \frac{A^{-1} \tilde{a}}{a} = \frac{1}{A^{-1} \tilde{a}} \left[ \tilde{a} \frac{dA^{-1}}{dt} + \frac{d\tilde{a}}{d\tilde{t}} \right] = -\frac{\dot{A}}{A} + A \tilde{H}, \quad (101)$$

where time deviation is taken with respect to  $t$ , as we want to express all physical quantities in the Einstein frame without reference to the Jordan frame. We also have the following important relations:

$$\dot{\tilde{\rho}} = \frac{d\tilde{\rho}}{d\tilde{t}} = A^{-1} \frac{1}{dt} (A^{-4} \rho_{\nu}) = -4A^{-5} \frac{\dot{A}}{A} \rho_{\nu} + A^{-5} \dot{\rho}_{\nu} \quad (102)$$

Using Equations (101) and (102), the continuity Equation (97) is transformed to the Einstein frame:

$$\dot{\rho}_{\nu} + 3H(\rho_{\nu} + p_{\nu}) = \frac{\dot{A}}{A} (\rho_{\nu} - 3p_{\nu})$$

or equivalently

$$\dot{\rho}_\nu + 3H\rho_\nu(1 + w_\nu) = \frac{A,\phi}{A}\dot{\phi}\rho_\nu(1 - 3w_\nu) \quad (103)$$

In a similar way, we derive the Klein–Gordon equation for the scalar field,

$$\ddot{\phi} + 3H\dot{\phi} + V_{,\phi} = -\frac{A,\phi}{A}(-\rho_\nu + 3p_\nu) \equiv -\frac{A,\phi}{A}\rho_\nu(1 - 3w_\nu), \quad (104)$$

which, after multiplying on both sides by  $\dot{\phi}$ , can be cast in the following suggestive form:

$$\dot{\rho}_\phi + 3H\rho_\phi(1 + w_\phi) = -\frac{A,\phi}{A}\dot{\phi}\rho_\nu(1 - 3w_\nu). \quad (105)$$

It is evident from Equations (103) and (105) that the conservation law does not hold for the neutrinos and scalar field individually but the total energy density,  $\rho_\phi + \rho_\nu$ , adheres to standard conservation as it should be.

Let us emphasise that neutrinos, due to their tiny masses ( $m_\nu = \mathcal{O}(10^{-2})$  eV), remain relativistic for most of the cosmic history with  $w_\nu = \frac{1}{3}$  and their coupling to the scalar field vanishes. Only at the late times, when they turn non-relativistic, do they start behaving as cold matter and the effect of the coupling comes into play, which has very interesting implications for late time dynamics. For a runaway type potential of the form (69), we argue that coupling modifies the potential such that the effective potential has a minimum around the present epoch. In the case of  $n = 1$ , we shall demonstrate analytically that the field settles in the minimum, giving rise to a quasi de Sitter-like behaviour that is exactly followed by massive neutrino matter. Numerical investigations confirm that the same conclusions hold for  $n > 1$ .

Let us first begin from general considerations. Owing to the non-relativistic nature of neutrinos around the present epoch, we can approximate by  $w_\nu \approx 0$ . It is further convenient for analytical estimation that we choose  $\hat{\rho}_\nu \equiv A^{-1}\rho_\nu$ , which is conserved in the Einstein frame,

$$\dot{\hat{\rho}}_\nu + 3H\hat{\rho}_\nu = 0, \quad (106)$$

and the field evolution equation in the approximation under consideration acquires the following form:

$$\ddot{\phi} + 3H\dot{\phi} = -V_{,\phi} - A_{,\phi}\hat{\rho}_\nu, \quad (107)$$

It is indicative from Equation (107) that we can write an effective potential, up to an additive constant, as

$$V_{\text{eff}} = V(\phi) + A(\phi)\hat{\rho}_\nu. \quad (108)$$

Let us now use a specific form of the conformal factor,

$$A(\phi) = e^{\alpha\gamma\frac{\phi}{M_{\text{Pl}}}}. \quad (109)$$

Although the original potential is runaway type with the chosen form of  $A(\phi)$ , the effective potential does possess a minimum; see Figure 5. It should be noted here that Equations (106) and (107) are exact for coupling to ordinary cold dark matter ( $w = 0$ ), whereas the equations hold only at late times when  $w_\nu \approx 0$  in the case of coupling to massive neutrino matter. To capture the behaviour of massive neutrino matter, which is relativistic at early times and non-relativistic near the present (late time), we assume the following ansatz:

$$w_\nu = \frac{1}{6} \left\{ 1 + \tanh \left[ \frac{\ln(1+z) - z_{\text{eq}}}{z_{\text{dur}}} \right] \right\}, \quad (110)$$

where  $z$  is the red shift and  $z_{\text{dur}}$  and  $z_{\text{equal}}$  are two parameters to be fixed using fitting with observation.

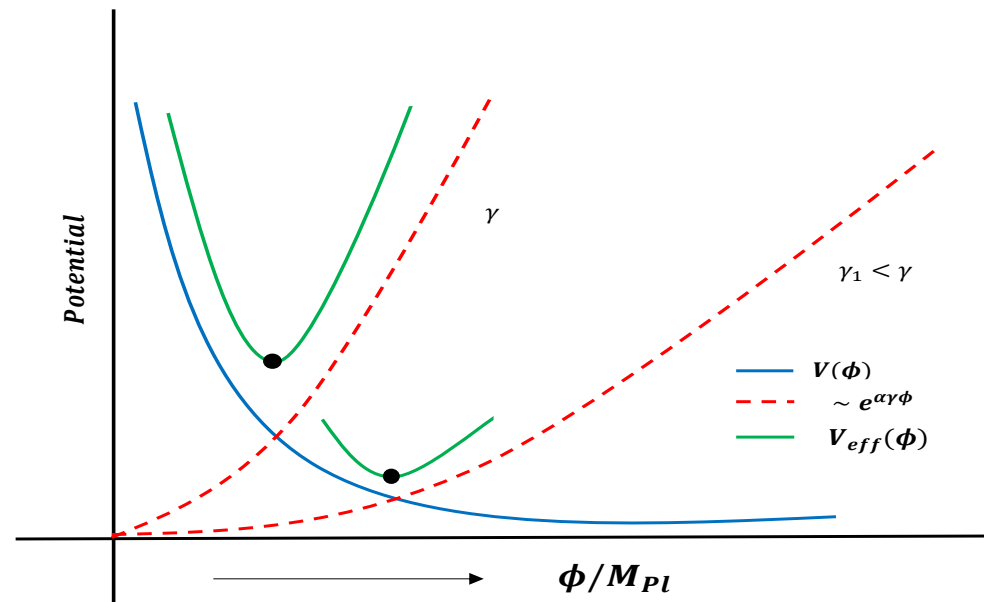


**Figure 5.** Schematic diagram showing the effective potential (green line); the original runaway type of potential is depicted by blue line. Coupling of field  $\phi$  to massive neutrino matter manifests itself in the effective potential (108) through  $A(\phi)\hat{\rho}_\nu$  [ $A(\phi) = \text{Exp}(\alpha\gamma\phi/M_{\text{Pl}})$ ], shown by dashed lines. The graph shows that for smaller values of  $\gamma$ , the minimum of effective potential hits larger values of the field.

The above applies to any runaway type of potential. However, in order to proceed further with analytical estimates, we shall consider the exponential potential (35) or (69) with  $n = 1$ . In this case, we have the expression for the effective potential:

$$V_{\text{eff}} = V_0 e^{-\alpha \frac{\phi}{M_{\text{Pl}}}} + \hat{\rho}_\nu e^{\alpha\gamma \frac{\phi}{M_{\text{Pl}}}} \quad (111)$$

Minimising the potential with regard to  $\phi$ , we find

$$\phi_{\text{min}} = \log\left(\frac{V_0}{\gamma\hat{\rho}_\nu}\right)^{\frac{M_{\text{Pl}}}{\alpha(1+\gamma)}} \implies V_{\text{eff,min}} = V_0 \left(\frac{\gamma\hat{\rho}_\nu}{V_0}\right)^{\frac{1}{1+\gamma}}, \quad (112)$$

where the potential (111) is defined up to an additive constant and the above relation is true for large values of  $\gamma$  required by observation (to be discussed below). The parameter  $\Gamma$  for the effective potential is shown in Figure 6. The question thus arises of whether the minimum given by (112) corresponds to the present dark energy density of the Universe. We will demonstrate that it does. It is instructive to rewrite Equations (103) and (104) for the conformal coupling (109),

$$\dot{\rho}_\nu + 3H\rho_\nu(1 + w_\nu) = \frac{\alpha\gamma}{M_{\text{Pl}}}\dot{\phi}\rho_\nu(1 - 3w_\nu) \quad (113)$$

$$\ddot{\phi} + 3H\dot{\phi} + V_{,\phi} = -\frac{\alpha\gamma}{M_{\text{Pl}}}\rho_\nu(1 - 3w_\nu), \quad (114)$$

Using the effective potential picture, which is approximate in the case of coupling to massive neutrino matter, we have put forward a general perspective to convince the reader that the coupling under consideration triggers transit to late time acceleration. In what

follows, we present the exact analytical results based upon dynamical analysis. Indeed, in this case, the autonomous system admits an attractor solution which corresponds to [167]

$$w_\phi = \frac{-3 + \alpha^2(1 + \gamma)}{\alpha^2(1 + \gamma)^2}, \quad (115)$$

$$\dot{\phi} = \frac{3HM_{\text{Pl}}}{\alpha(1 + \gamma)}. \quad (116)$$

It is interesting to check for the late time behaviour of neutrino matter density. One might naively think that with the field approaching de Sitter,  $\dot{\phi} \rightarrow 0$  and  $w_\nu \approx 0$  near the present epoch, neutrino matter should decouple from the scalar field and  $\rho_\nu \sim a^{-3}$ ; see Equation (113). On the contrary,  $\rho_\nu$  follows the scalar field and behaves as dark energy, which is counter-intuitive. This behaviour can be understood recalling Equation (103), and the fact that  $p_\nu \approx 0$  around the present epoch. Indeed,

$$\dot{\rho}_\nu + 3H\rho_\nu \left(1 - \frac{A, \phi}{A} \frac{\dot{\phi}}{3H}\right) = 0. \quad (117)$$

Taking into account that  $A, \phi/A = \alpha\gamma/M_{\text{Pl}}$ , we write the continuity equation in a suggestive form,

$$\dot{\rho}_\nu + 3H(1 + w_\nu^{\text{eff}}) = 0; \quad w_\nu^{\text{eff}} \equiv -\frac{\alpha\gamma\dot{\phi}}{3HM_{\text{Pl}}} \quad (118)$$

The behaviour of  $w_\nu^{\text{eff}}$  determines the late time evolution of neutrino matter density. Indeed, plugging  $\dot{\phi}$  from Equation (116) into Equation (118), we get

$$w_\nu^{\text{eff}} = -\frac{\alpha\gamma\dot{\phi}}{3HM_{\text{Pl}}} = -\frac{\gamma}{1 + \gamma}. \quad (119)$$

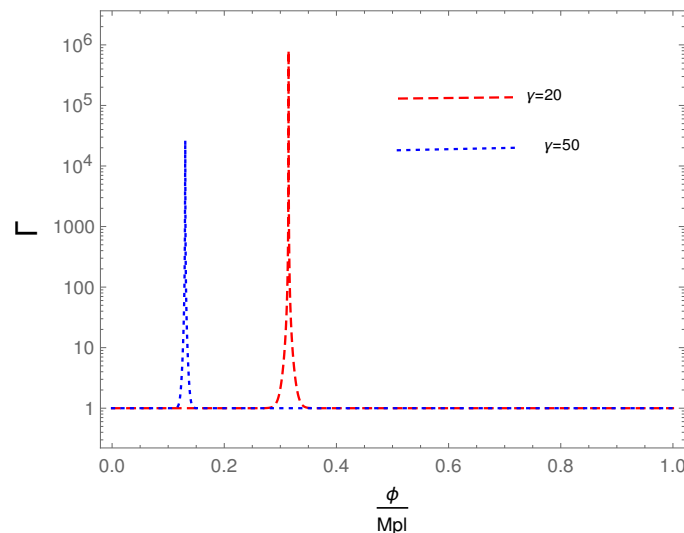


**Figure 6.** Figure shows the plot of  $\Gamma$  for effective potential given by (111).  $\Gamma$  increases rapidly during slow roll, which happens here around the minimum, which shifts towards larger values of  $\phi$  for smaller values of  $\gamma$ . The plot is for  $\alpha = 10$  and the potential is normalised by  $V_0$ .

In fact, numerical results confirm that the same features are shared by the model based upon the generalised exponential potential (69); see Figures 7 and 8, and Ref. [115] for details. In terms of the effective potential picture, it is clear that the minimum is time-dependent via  $\hat{\rho}_\nu$ , but the system essentially settles around its attractor and matches observational values of the dark energy paradigm at the present epoch by appropriately choosing “ $\gamma$ ”.

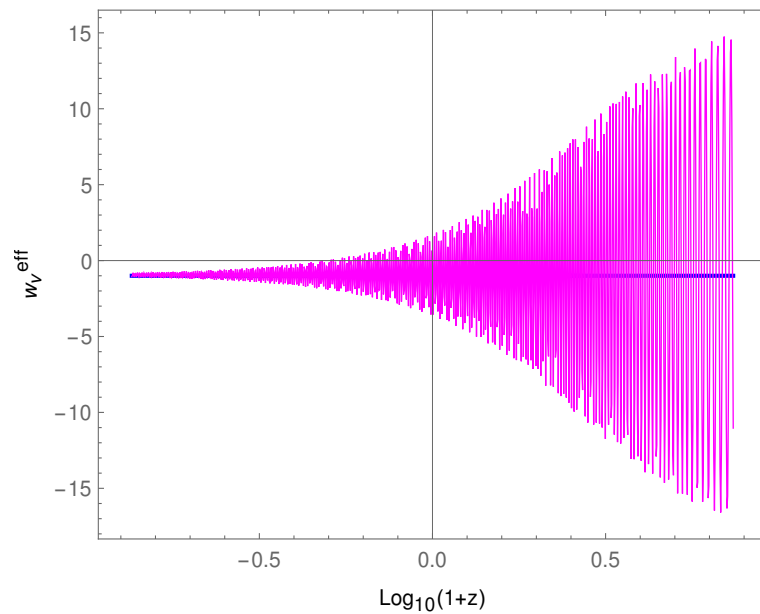


**Figure 7.** Evolution of  $w_v^{\text{eff}}$  versus the red shift in case of the generalised exponential potential (69) for  $n = 3$  and  $\alpha\gamma = 1000$ , compatible with observation [115]; solid blue line corresponds to  $w_v^{\text{eff}} = -1$ . Figure shows that  $w_v^{\text{eff}}$  oscillates and eventually settles close to minus one.

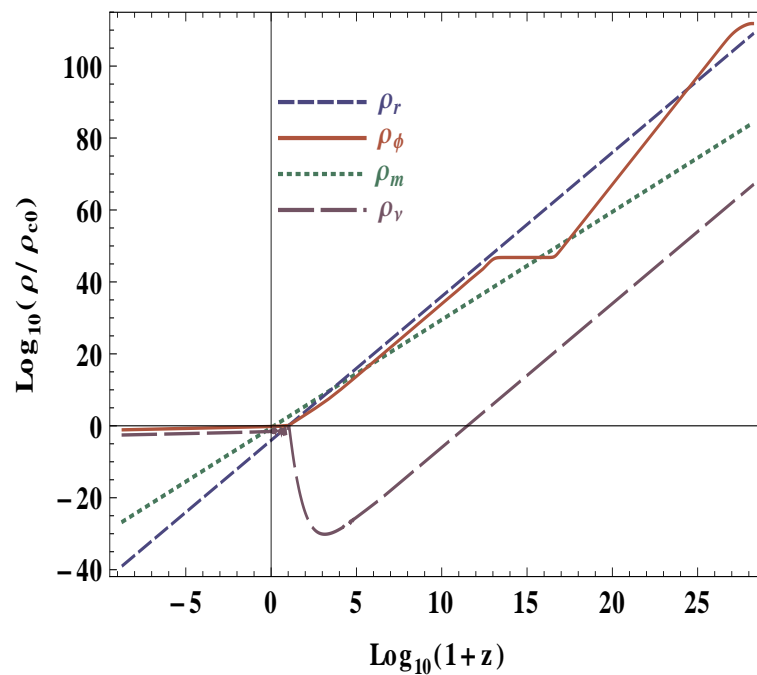


**Figure 8.** Plot of energy densities versus the red shift on the log scale for generalised exponential potential (69). Evolution is shown from the end of inflation. Field is shown to track the background with exit to de Sitter at late times followed by the massive neutrino matter density. Figure corresponds to numerical values of parameters:  $\gamma = 800$ ,  $\lambda = 10^{-8}$ ,  $n = 6$ ,  $z_{\text{eq}} = 2.55$  &  $z_{\text{dur}} = 3$ .

A comment on the coupling of the scalar field to dark matter is in order. In this case, the exit to acceleration might happen soon after matter domination is established. The only free parameter  $\gamma$  should then be tuned to delay the minimum to the late stage, which is accomplished by taking a  $\gamma \ll 1$  (see Figures 5 and 6) but this defies acceleration as  $w_\phi \rightarrow 0, \gamma \rightarrow 0$  and the system is back to scaling track. We have demonstrated that this issue is successfully addressed by invoking coupling to massive neutrino matter.

Let us summarise our main findings in this sub-section. Scalar field coupling to massive neutrino matter, due to tiny neutrino masses, builds up dynamically only at late stages, giving rise to an exit from the scaling regime to a de Sitter-like configuration around the present epoch. In the case of exponential potential, we support our conclusions with analytical estimates. Indeed, in this case, as  $\gamma$  becomes larger and larger,  $\dot{\phi}$  becomes smaller and smaller ( $\dot{\phi} \rightarrow 0$ ) such that  $\alpha\gamma\dot{\phi} \sim H_0 M_{\text{Pl}} \sim \rho_{\text{cr}}^{1/2}$  and the RHS of Equation (113) is non-vanishing as de Sitter is approached. As a result, neutrino matter is never decoupled from the scalar field while de Sitter is approached. The latter forces the neutrino matter to follow the scalar field at late times. Numerical results confirm the same behaviour for  $n > 1$ ; see Figure 8.

### 5. The Distinguished Features of Quintessential Inflation: Relic Gravity Waves

The gravity waves (GW) are described by the transverse traceless component of the metric perturbation over the background space time, e.g., especially flat FLRW space time,  $ds^2 = -dt^2 + a(t)^2 (h_{ij} + \delta_{ij}) dx^i dx^j$ . The perturbation satisfies the transverse traceless condition  $h_i^i = 0, \partial_i h^i = 0$ . The Fourier decomposition for the perturbation for a mode with wave number  $\mathbf{k}$  can be written as

$$h_{ij}(t, x) = \sum_{n=+, \times} \int \frac{d\mathbf{k}}{(2\pi)^{2/3}} \varphi_{ij}^n(\mathbf{k}) h_{\mathbf{k}}^n(k, t) e^{i\mathbf{k}\cdot\mathbf{x}}, \quad (120)$$

where the polarisation tensor  $\varphi_{ij}^n(\mathbf{k})$  is symmetric and satisfies the transverse traceless condition. The Fourier component of the tensor mode satisfies the wave equation [169]

$$h_{\mathbf{k}}^{n''}(\tau) + 2\frac{a'}{a} h_{\mathbf{k}}^{n'}(\tau) + k^2 h_{\mathbf{k}}^n = 0, \quad (121)$$

where the  $'$  denotes the derivative with respect to conformal time,  $d\tau \equiv \frac{dt}{a}$ . The energy spectrum for the GWs with wave number  $k$  is given by

$$\Omega_{\text{GW}}(k, \tau) \equiv \frac{1}{\rho_{\text{cr}}} \frac{d\rho_{\text{GW}}}{d \ln k}. \quad (122)$$

The GW energy density is given by

$$\rho_{\text{GW}} = -T_0^0 = \frac{M_{\text{Pl}}^2}{4} \int \frac{d^3k}{(2\pi)^3} \frac{k^2}{a^2} 2 \sum_n |h_{\mathbf{k}}^n|^2. \quad (123)$$

The GW energy spectrum for the present time can be written as

$$\Omega_{\text{GW},0} = \frac{1}{12} \left( \frac{k^2}{a_0^2 H_0^2} \right) P_T(k) T^2(k), \quad (124)$$

where  $P_T(k) = \frac{2}{\pi^2} \frac{H_{\text{inf}}^2}{M_{\text{Pl}}^2} \Big|_{k=aH}$  is the primordial tensor power spectrum, defined at the horizon crossing, and  $T^2(k)$  is the transfer function that describes the time evolution of each mode after the end of inflation. The transfer function today is given by [170–172].

$$T^2(k) = \frac{1}{2} \frac{a_{\text{hc}}^2}{a_0^2}, \quad (125)$$

where the subscript “0” represents the value at the present time and hc for horizon crossing. Here, it should be mentioned that in the super-horizon limit  $k \ll aH$ ,  $h_{\mathbf{k}}$  stays constant and varies as  $h_{\mathbf{k}} \propto \frac{1}{a}$  in the sub-horizon limit,  $k \gg aH$ . Different modes of GW enter the horizon at different epochs, and to evaluate the spectrum today, we need to calculate the Hubble parameter precisely:

$$H \approx H_0 \sqrt{\Omega_\phi(a) + \Omega_{r0} \left(\frac{g^*}{g_{*0}}\right) \left(\frac{g_{*s}}{g_{*s0}}\right)^{-4/3} \left(\frac{a}{a_0}\right)^{-4} + \Omega_{m0} \left(\frac{a}{a_0}\right)^{-3}}, \quad (126)$$

where  $g_*(s)$  denotes the effective number of relativistic degrees of freedom at temperature  $T$  contributing to entropy. It should be mentioned that the major contribution of the scalar field to Hubble comes in two phases, namely the kinetic regime, which follows inflation, and the dark energy era around the present epoch. Let us put it in the following form:

$$\Omega_\phi(a) = \Omega_{\phi K} + \Omega_{\Lambda 0}, \quad (127)$$

where the latter is identified with the present value of dark energy. The kinetic part can be evaluated as

$$\Omega_{\phi,K} \equiv \frac{\rho_{\phi,K}}{3H_0^2 M_{\text{Pl}}^2} = \frac{\rho_{\phi,\text{end}}}{3H_0 M_{\text{Pl}}^2} \left(\frac{a}{a_{\text{end}}}\right)^{-6} = \frac{3H_{\text{end}}^2 M_{\text{Pl}}^2}{3H_0^2 M_{\text{Pl}}^2} \left(\frac{a}{a_{\text{end}}}\right)^{-6} = \frac{H_{\text{end}}^2}{H_0^2} \left(\frac{a}{a_{\text{end}}}\right)^{-6}. \quad (128)$$

Making use of the relation  $k = a_{\text{hc}} H_{\text{hc}}$  and Equation (126), the scale factor  $a_{\text{hc}}$  in different regimes, can be expressed as

$$a_{\text{hc,MD}} = \frac{H_0^2 a_0^3}{k^2} \Omega_{m0} \quad (129)$$

$$a_{\text{hc,RD}} = \frac{a_0^2 H_0}{k} \left(\frac{g^*}{g_{*0}}\right)^{1/2} \left(\frac{g_{*s}}{g_{*s0}}\right)^{-2/3} \sqrt{\Omega_{r0}} \quad (130)$$

The scale factor for those modes entering during the kinetic epoch can be found by using the fact that, during a kinetic epoch, up to the radiation commencement, the energy density is  $\rho_{\text{tot}} \approx \rho_\phi \propto a^{-6}$  (or equivalently  $H \propto a^{-3}$ ) and  $k_r = H_r a_r$

$$\begin{aligned} k &= a_{\text{hc,KD}} H_{\text{hc}} = \frac{a_{\text{hc,KD}} H_{\text{hc}}}{a_r H_r} a_r H_r = \frac{a_{\text{hc,KD}} H_{\text{end}} \left(\frac{a_{\text{end}}}{a_{\text{hc,KD}}}\right)^3}{a_r H_{\text{end}} \left(\frac{a_{\text{end}}}{a_r}\right)^3} k_r \\ &= \frac{a_r^2}{a_{\text{hc,KD}}^2} \implies \frac{a_{\text{hc,KD}}}{a_r} = \left(\frac{k_r}{k}\right)^{1/2}. \end{aligned} \quad (131)$$

Substituting the values of the scale factors (129)–(131) to the transfer function (125), we obtain

$$\Omega_{\text{GW},0}^{(\text{MD})} = \frac{1}{6\pi^2} \Omega_{m0}^2 \frac{H_{\text{inf}}^2}{M_{\text{Pl}}^2} \frac{a_0^2 H_0^2}{k^2} \quad \text{for } (k_0 < k < k_{\text{eq}}) \quad (132)$$

$$\Omega_{\text{GW},0}^{(\text{RD})} = \frac{1}{6\pi^2} \Omega_{r0} \frac{H_{\text{inf}}^2}{M_{\text{Pl}}^2} \left(\frac{g^*}{g_{*0}}\right) \left(\frac{g_{*s}}{g_{*s0}}\right)^{-4/3} \quad \text{for } (k_{\text{eq}} < k < k_r) \quad (133)$$

$$\Omega_{\text{GW},0}^{(\text{KD})} = \Omega_{\text{GW},0}^{(\text{RD})} \left(\frac{k}{k_r}\right) \quad \text{for } (k_{\text{end}} < k < k_r) \quad (134)$$

where  $k_0$ ,  $k_{\text{eq}}$ ,  $k_{\text{end}}$ ,  $k_r$  represent values of  $k$  at present, matter–radiation equality, end of inflation and commencement of the radiation era, respectively. The corresponding frequencies can easily be evaluated using the relation  $f = \frac{aH}{2\pi}$

$$f_0 = \frac{a_0 H_0}{2\pi} \sim 3 \times 10^{-19} \text{ Hz} \quad (135)$$

$$f_{\text{eq}} = \frac{a_{\text{eq}} H_{\text{eq}}}{2\pi} \sim 10^{-17} \text{ Hz} \quad (136)$$

$$f_{\text{end}} = \frac{a_{\text{end}} H_{\text{end}}}{2\pi} = \frac{T_0}{T_{\text{end}}} \left(\frac{43}{11g_{*s}}\right)^{1/3} \frac{H_{\text{end}}}{2\pi} \gtrsim 10^8 \text{ Hz} \quad (137)$$

In the last step, we have given a lower bound on the frequency at the end of inflation in a model-independent way by considering instantaneous energy transfer at reheating. The gravitational wave spectrum is shown in Figure 9.

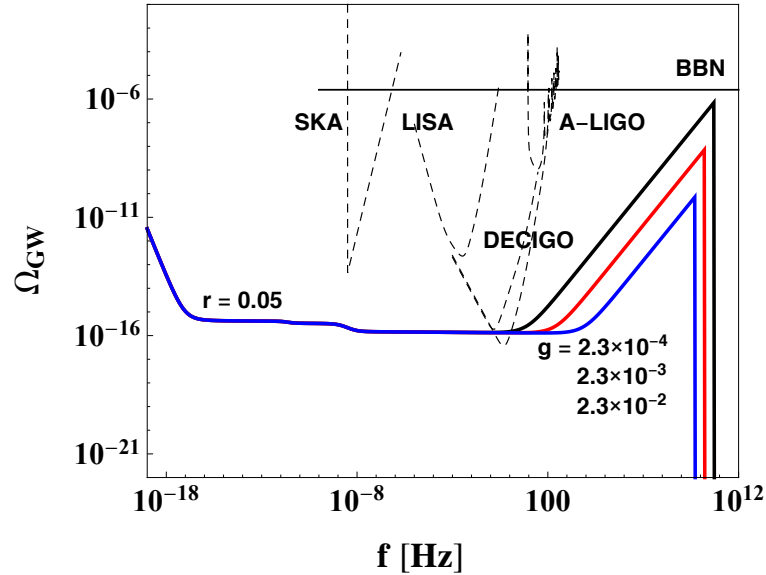


**Figure 9.** The GW spectrum versus the frequency in Hz for the paradigm of quintessential inflation. The blue tilt in the spectrum is visible on the high-frequency side due to the presence of a long kinetic epoch. Instant preheating is assumed as the reheating mechanism with coupling constant  $g$  (consistent with nucleosynthesis constraint); see Section 2.2 and Ref. [173].

#### Nucleosynthesis Constraint on Reheating Temperature

As discussed in Section 3.4, the presence of any relativistic degree of freedom in the Universe, over and above the standard model of particle physics, is subject to the nucleosynthesis constraint. In particular, we have a bound on relic gravity waves given by (50). Since the major contribution to the GW spectrum comes from the blue-tilted spectrum due to the kinetic regime ( $k_{\text{end}} < k < k_r$ ), we have [149,174]

$$\Omega_{\text{GW},0} \simeq \Omega_{\text{GW},0}^{\text{KD}} \equiv \Omega_{\text{GW},0}^{(\text{max})} < 1.12 \times 10^{-6} \quad (138)$$

Substituting the value of  $\Omega_{\text{GW},0}^{(\text{KD})}$  from Equation (134), and using the fact that, for the highest frequency at the kinetic epoch,  $a = a_{\text{kin}} \approx a_{\text{end}}$ , we get

$$\Omega_{\text{GW},0}^{\text{max}} = \frac{1}{6\pi^2} \Omega_{r0} \frac{H_{\text{inf}}^2}{M_{\text{Pl}}^2} \frac{g_*}{g_{*0}} \left( \frac{g_{*s}}{g_{*s0}} \right)^{-\frac{4}{3}} \left( \frac{a_r}{a_{\text{end}}} \right)^2 \quad (139)$$

Putting the values  $\Omega_{r0} = 9.24 \times 10^{-5}$ ,  $g_*(a_{\text{end}}) = g_{*s}(a_{\text{end}}) = 106.75$ ,  $g_{*0} = 3.36$ ,  $g_{*s0} = 3.91$ ;  $H_{\text{inf}} = 1.4 \times 10^{14} r^{\frac{1}{2}}$  GeV and using the upper bound on the tensor to scalar ratio of perturbations,  $r \approx 0.05$ , we obtain the upper bound on the GW spectrum,

$$\Omega_{\text{GW},0}^{\text{max}} = 3.8 \times 10^{-16} \left( \frac{a_r}{a_{\text{end}}} \right)^2 = 3.8 \times 10^{-16} \left( \frac{T_{\text{end}}}{T_r} \right)^2 \quad (140)$$

$$\Omega_{\text{GW},0}^{\text{max}} < 1.12 \times 10^{-6} \implies \left( \frac{T_{\text{end}}}{T_r} \right) < 5.5 \times 10^4. \quad (141)$$

where we have used the relation  $a_r/a_{\text{end}} = T_{\text{end}}/T_r$ . This bound enables us to constrain the duration of the kinetic regime: from the end of inflation to the commencement of the radiation era. The higher is the radiation energy density produced at the end of inflation,

the shorter would be the kinetic regime and the easier it would be to comply with the BBN bound. Let us consider a natural mechanism dubbed gravitational particle production and check for its consistency with nucleosynthesis. In gravitational reheating (see Section 2.1), the energy density produced after the end of inflation is given by

$$\rho_{r,\text{end}} = 10^{-2} g_p H_{\text{end}}^4 \approx 1.15 \times 10^{-17} M_{\text{Pl}}^4 r, \quad (142)$$

where, in the last step, we used  $g_p = 100$ . From Equation (19), we have  $\rho_{\phi,\text{end}} \approx 1 \times 10^{-8} M_{\text{Pl}}^4 r^2$ . Thus, Equation (22) yields

$$\left( \frac{a_r}{a_{\text{end}}} \right)^2 = \left[ \frac{\rho_{\phi,\text{end}}}{\rho_{\text{end}}} \right] \approx 1.8 \times 10^{10}. \quad (143)$$

Finally, using Equation (140), we arrive at the following estimate

$$\Omega_{\text{GW},0}^{\text{max}} \approx 6 \times 10^{-6}, \quad (144)$$

which challenges the nucleosynthesis constraint (50). This is attributed to the inefficiency (smaller value of  $\rho_{r,\text{end}}$  and correspondingly larger value of  $(\rho_{\phi}/\rho_r)_{\text{end}}$ ) of the reheating process based upon gravitational particle production [173]. In fact, other reheating mechanisms can give rise to larger values of  $\rho_{r,\text{end}}$ , circumventing the problem due to relic gravity waves. For example, in an instant preheating scenario, we have  $(\rho_{\phi}/\rho_r)_{\text{end}} = (2\pi)^3/g^2$ , with  $g$  being a coupling constant in the scenario. Constraining  $g$ , one can easily comply with the nucleosynthesis bound; see Ref. [173] for details.

## 6. Summary

This review is a pedagogical exposition of scalar field dynamics in the FLRW background applied to quintessential inflation. In this framework, two specific roles are assigned to a scalar field, namely a consistent description of inflation and late time acceleration, with the understanding that the field is invisible starting from the commencement of the radiative regime till the beginning of late time acceleration. The other important demand from scalar field dynamics is related to the insensitivity of late time physics concerning the initial (field) conditions. These requirements broadly characterise the class of scalar field potentials suited to the framework under consideration: potentials that are flat initially, followed by steep behaviour in the post-inflationary era, and again flat around the present epoch. Without loss of generality, one assumes that the runaway potential is such that the field rolls away from the origin towards plus infinity. After inflation ends, the field energy density  $\rho_{\phi}$  is larger by several orders of magnitude than the energy density of radiation assumed to be produced due to some alternative mechanism. Consequently, the field evolves in the kinetic regime for a long time before the commencement of radiation domination. Following this,  $\rho_{\phi}$  overshoots the background matter (radiation) density such that  $\rho_{\phi} \ll \rho_r$ . The field then freezes on its potential due to Hubble damping and waits till the radiation density red-shifts to the level where  $\rho_r/\rho_{\phi}$  becomes comparable to  $\lambda_s^2/2$  ( $\lambda_s$  is the slope of steep potential). Hereafter, the field dynamics are sensitive to the type of steepness of the potential, which is quantified by the parameter  $\Gamma$ . If  $\Gamma = 1$  (exponential potential), the field exactly follows the background as the scaling solution is an attractor in this case. In the case of  $\Gamma > 1$ —for instance, inverse power law potentials ( $V \sim \phi^{-n}$ ,  $\Gamma = 1 + 1/n$ )—the slope decreases such that the field nearly follows the background while evolving along the steep part of the potential and at late times enters the slow roll regime. This class of potentials is suitable for tracker behaviour. Slope, on the other hand, increases with evolution if  $\Gamma < 1$  and, in this case,  $\Gamma$  eventually approaches its scaling value in the asymptotic region. We demonstrated that the generalised exponential potential that falls in this class gives rise to a scaling solution in the asymptotic regime, which is an attractor. This class of potentials, shallow initially, is suitable for inflation and, in the post-inflationary era, retains the characteristics of a steep exponential potential. We further demonstrated that a perfect

tracker can be designed from the classes of potentials with  $\Gamma \leq 1$  by invoking a late time feature in the potentials that could facilitate exit to acceleration. In the case of  $\Gamma = 1$ , we also need to invoke an early time feature in the potential, which, in particular, can be achieved using a non-canonical kinetic term in the scalar field Lagrangian.

As for the exit to late time acceleration, we mentioned different ways to realise it and presented detailed investigations of a mechanism based upon the coupling of the field to massive neutrino matter. In this framework, the distinguished physical process in the late Universe, namely the transformation of massive neutrinos from relativistic to non-relativistic, can trigger the desired exit.

The focus in this review was on the building blocks of quintessential inflation rather than the concrete models. We emphasised the model-independent and generic features of the paradigm. For instance, a long kinetic regime after the end of inflation and before the commencement of a radiative regime is an essential component of the framework, which distinguishes it from the standard inflationary scenario. The latter induces a novel feature in the spectrum of relic gravity waves, namely a blue-tilted spectrum in the high-frequency regime. To this effect, we have included a brief discussion on relic gravity waves and presented the model-independent estimates to highlight the distinguishing features of the paradigm.

Last but not least, our discussion, especially on scalar field dynamics in the post-inflationary era, is pedagogical, and we hope that the review will be helpful for young researchers interested in topics related to quintessential inflation and dark energy.

**Author Contributions:** Both authors M.S. and N.J. have equally contributed to all and every aspects for this article. All authors have read and agreed to the published version of the manuscript.

**Funding:** M.S. is partially supported by the Ministry of Education and Science of the Republic of Kazakhstan, Grant No. 0118RK00935. N.J. is supported by the National Postdoctoral Fellowship of the Science and Engineering Research Board (SERB), Department of Science and Technology (DST), Government of India, File No. PDF/2021/004114.

**Institutional Review Board Statement:** Not applicable.

**Informed Consent Statement:** Not applicable.

**Data Availability Statement:** Not applicable.

**Acknowledgments:** We thank V. Sahni, R. Gannouji, Anzhong Wang, Shibesh Kumar, S. Capozziello, Azam Mofazzal and Sang Pyo Kim for their useful comments. We are indebted to Konstantinos Dimopoulos for his invitation to write this review and for making valuable comments that allowed us to improve the draft. N.J. thanks the Centre for Cosmology and Science Popularisation (CCSP), SGT University, for their hospitality, where the work was initiated.

**Conflicts of Interest:** The authors declare no conflict of interest.

## Notes

- <sup>1</sup> In this framework, field  $\phi$  is coupled to another scalar field  $\chi$ , which in turn couples to matter fields:  $\mathcal{L}_{int} = -(1/2)g^2\phi^2\chi^2 - h\chi\bar{\Psi}\Psi$ . In this case,  $\chi$  does not bear mass; its effective mass depends upon  $\phi$ ,  $m_\chi = g\phi$ . After inflation, as  $\phi$  runs down its potential rapidly,  $m_\chi$  changes in a non-adiabatic fashion, giving rise to the production of  $\chi$  particles, which might instantaneously decay into matter fields. Assuming that the energy of the produced particles is instantaneously thermalised (denoted by  $\rho_r$ ), one finds at the end of inflation that  $(\rho_\phi/\rho_r)_{end} = (2\pi)^3/g^2$ .
- <sup>2</sup> Expansion has character of acceleration ( $\ddot{a}/a > 0$  for  $w_\phi < -1/3$ ); see Equation (5).
- <sup>3</sup> The acceleration term,  $\ddot{\phi}$  in (8), can no longer be dropped in the case of a steep potential.
- <sup>4</sup> It might look more natural to use the variable  $X$  and  $Y$  as we know their values for the scaling solution. However, in this case, one requires one more variable,  $A$ , which is directly linked to the field  $\phi$ . However, the equation for this variable decouples from the system and we can analyse equations for  $X$  and  $Y$  without bothering about the third equation for the variable  $A$ . These variables are useful in the analysis of asymptotic scaling solutions that occur in the case of steep potentials of variable slope, where we have a system of three coupled equations for  $X$ ,  $Y$  and  $A$ .
- <sup>5</sup> Given that  $\Delta N_\nu$  is constrained using primordial abundances and other data, bound (45) is referred to as a “nucleosynthesis” constraint or “BBN” bound.

- 6 Notice that  $w_\phi = w_b$  for  $n \rightarrow \infty$ , which is not surprising as the power law corresponds to exponential in this limit.
- 7 We skip details here and refer the reader to [130] for the same.
- 8 It should be noted that, in the present situation,  $-\dot{H}/H^2 = (1 + w_b)/2$  is not related to the slow roll parameter due to the presence of background matter. In the case of slowly rolling quintessence, the friction term need not to be large and  $\beta$  may not be negligible. For tracker models,  $|\beta| \ll 1$ ; however, for thawing quintessence,  $\beta = \mathcal{O}(1)$ , and  $\beta$  is nearly constant,  $\beta/\beta H \ll 1$ . Unlike the thawing case, the consistency of slow roll gives rise to  $\eta = 3(1 + w_b)/2 = 3/2$  in the case of the trackers.
- 9 Let us note that this feature is central to thawing models where the field is frozen on a shallow potential such that the field begins slow roll after it recovers from Hubble damping and accounts for late time acceleration. Initial conditions are set specially or tuned, allowing it to happen around the present epoch, and model parameters are chosen to comply with observation
- 10  $\dot{\phi}^2/2 = 2V, V$  for radiation and matter domination, respectively.
- 11 One should be careful here with regard to  $\Gamma$ , which is one for exponential potential, irrespective of its being steep or shallow.

## References

1. Aghanim, N.; Akrami, Y.; Ashdown, M.; Aumont, J.; Baccigalupi, C.; Ballardini, M.; Banday, A.J.; Barreiro, R.B.; Bartolo, N.; Basak, S.; et al. Planck 2018 results. VI. Cosmological parameters. *Astron. Astrophys.* **2020**, *641*, A6, Erratum in *Astron. Astrophys.* **2021**, *652*, C4. [[CrossRef](#)]
2. Guth, A.H. Inflationary universe: A possible solution to the horizon and flatness problems. *Phys. Rev. D* **1981**, *23*, 347–356. [[CrossRef](#)]
3. Sato, K. First Order Phase Transition of a Vacuum and Expansion of the Universe. *Mon. Not. R. Astron. Soc.* **1981**, *195*, 467–479. [[CrossRef](#)]
4. Linde, A.D. A New Inflationary Universe Scenario: A Possible Solution of the Horizon, Flatness, Homogeneity, Isotropy and Primordial Monopole Problems. *Phys. Lett. B* **1982**, *108*, 389–393. [[CrossRef](#)]
5. Albrecht, A.; Steinhardt, P.J. Cosmology for Grand Unified Theories with Radiatively Induced Symmetry Breaking. *Phys. Rev. Lett.* **1982**, *48*, 1220–1223. [[CrossRef](#)]
6. Starobinsky, A.A. A new type of isotropic cosmological models without singularity. *Phys. Lett. B* **1980**, *91*, 99–102. [[CrossRef](#)]
7. Starobinsky, A.A. Dynamics of phase transition in the new inflationary universe scenario and generation of perturbations. *Phys. Lett. B* **1982**, *117*, 175–178. [[CrossRef](#)]
8. Liddle, A.R. An Introduction to cosmological inflation. *arXiv* **1999**, arXiv:astro-ph/9901124.
9. Tsujikawa, S. Introductory review of cosmic inflation. *arXiv* **2003**, arXiv:hep-ph/0304257.
10. Martin, J.; Ringeval, C.; Vennin, V. Encyclopædia Inflationaris. *Phys. Dark Univ.* **2014**, *5–6*, 75–235. [[CrossRef](#)]
11. Vázquez, J.A.; Padilla, L.E.; Matos, T. Inflationary Cosmology: From Theory to Observations. *Rev. Mex. Física E* **2020**, *17*, 73–91. [[CrossRef](#)]
12. Riess, A.G.; Filippenko, A.V.; Challis, P.; Clocchiatti, A.; Diercks, A.; Garnavich, P.M.; Gillil, R.L.; Hogan, C.J.; Jha, S.; Kirshner, R.P.; et al. Observational evidence from supernovae for an accelerating universe and a cosmological constant. *Astron. J.* **1998**, *116*, 1009–1038. [[CrossRef](#)]
13. Perlmutter, S.; Aldering, G.; Goldhaber, G.; Knop, R.A.; Nugent, P.; Castro, P.G.; Deustua, S.; Fabbro, S.; Goobar, A.; Groom, D.E.; et al. Measurements of  $\Omega$  and  $\Lambda$  from 42 high redshift supernovae. *Astrophys. J.* **1999**, *517*, 565–586. [[CrossRef](#)]
14. Hawking, S.W. The Development of Irregularities in a Single Bubble Inflationary Universe. *Phys. Lett. B* **1982**, *115*, 295. [[CrossRef](#)]
15. Bardeen, J.M.; Steinhardt, P.J.; Turner, M.S. Spontaneous Creation of Almost Scale-Free Density Perturbations in an Inflationary Universe. *Phys. Rev. D* **1983**, *28*, 679. [[CrossRef](#)]
16. Krauss, L.M.; Turner, M.S. The Cosmological constant is back. *Gen. Relativ. Gravit.* **1995**, *27*, 1137–1144. [[CrossRef](#)]
17. Turner, M.S. The Case for  $\Lambda$ CDM. *arXiv* **1997**, arXiv:astro-ph/9703161.
18. Netterfield, C.B.; Ade, P.; Bock, J.J.; Bond, J.R.; Borrill, J.; Boscaleri, A.; Coble, K.; Contaldi, C.; Crill, B.; de Bernardis, P.; et al. A measurement by Boomerang of multiple peaks in the angular power spectrum of the cosmic microwave background. *Astrophys. J.* **2002**, *571*, 604–614. [[CrossRef](#)]
19. Halverson, N.W. DASI first results: A Measurement of the cosmic microwave background angular power spectrum. *Astrophys. J.* **2002**, *568*, 38–45. [[CrossRef](#)]
20. Peebles, P.J.E.; Vilenkin, A. Quintessential inflation. *Phys. Rev. D* **1999**, *59*, 063505. [[CrossRef](#)]
21. Peebles, P.J.E.; Ratra, B. Cosmology with a Time Variable Cosmological Constant. *Astrophys. J. Lett.* **1988**, *325*, L17. [[CrossRef](#)]
22. Sahni, V.; Sami, M.; Souradeep, T. Relic gravity waves from brane world inflation. *Phys. Rev. D* **2002**, *65*, 023518. [[CrossRef](#)]
23. Huey, G.; Lidsey, J.E. Inflation, braneworlds and quintessence. *Phys. Lett. B* **2001**, *514*, 217–225. [[CrossRef](#)]
24. Majumdar, A.S. From brane assisted inflation to quintessence through a single scalar field. *Phys. Rev. D* **2001**, *64*, 083503. [[CrossRef](#)]
25. Dimopoulos, K. Towards a model of quintessential inflation. *Nucl. Phys. B Proc. Suppl.* **2001**, *95*, 70–73. [[CrossRef](#)]
26. Sami, M.; Dadhich, N.; Shiromizu, T. Steep inflation followed by Born-Infeld reheating. *Phys. Lett. B* **2003**, *568*, 118–126. [[CrossRef](#)]
27. Dimopoulos, K. Curvaton hypothesis and the  $\eta$  problem of quintessential inflation, with and without branes. *Phys. Rev. D* **2003**, *68*, 123506. [[CrossRef](#)]
28. Dias, M.; Liddle, A.R. On the possibility of braneworld quintessential inflation. *Phys. Rev. D* **2010**, *81*, 83515. [[CrossRef](#)]

29. Bastero-Gil, M.; Berera, A.; Jackson, B.M.; Taylor, A. Hybrid quintessential inflation. *Phys. Lett. B* **2009**, *678*, 157. [[CrossRef](#)]
30. Chun, E.J.; Scopel, S.; Zaballa, I. Gravitational reheating in quintessential inflation. *JCAP* **2009**, *22*, 907. [[CrossRef](#)]
31. Bento, M.C.; Felipe, R.G.; Santos, N.M.C. Brane assisted quintessential inflation with transient acceleration. *Phys. Rev. D* **2008**, *77*, 123512. [[CrossRef](#)]
32. Matsuda, T. NO curvatons or hybrid quintessential inflation. *JCAP* **2007**, *8*, 3. [[CrossRef](#)]
33. Neupane, I.P. Reconstructing a model of quintessential inflation. *Class. Quantum Gravity* **2008**, *25*, 125013. [[CrossRef](#)]
34. Dimopoulos, K. Trapped quintessential inflation from flux compactifications. *arXiv* **2007**, arXiv:hep-ph/0702018.
35. Gardner, C.L. Braneworld quintessential inflation and sum of exponentials potentials. *arXiv* **2007**, arXiv:hep-ph/0701036.
36. Sami, M.; Dadhich, N. World inflation with quintessence. *arXiv* **2004**, arXiv:hep-th/0405016.
37. Rosenfeld, R.; Frieman, J.A. Cosmic microwave background and large-scale structure constraints on a simple quintessential inflation model. *Phys. Rev. D* **2007**, *75*, 043513. [[CrossRef](#)]
38. Sanchez, J.C.B.; Dimopoulos, K. Trapped quintessential inflation in the context of flux compactifications. *JCAP* **2007**, *10*, 2. [[CrossRef](#)]
39. Membrilla, A.; Bellini, M. Quintessential inflation from a variable cosmological constant in a 5D vacuum. *Phys. Lett. B* **2006**, *641*, 125. [[CrossRef](#)]
40. Cardenas, V.H. Tachyonic quintessential inflation. *Phys. Rev. D* **2006**, *73*, 103512. [[CrossRef](#)]
41. Zhai, X.-h.; Zhao, Y.-b. Dynamics of quintessential inflation. *Chin. Phys.* **2006**, *15*, 2465. [[CrossRef](#)]
42. Rosenfeld, R.; Frieman, J.A. A simple model for quintessential inflation. *CAP* **2005**, *9*, 3. [[CrossRef](#)]
43. Giovannini, M. Low-scale quintessential inflation. *Phys. Rev. D* **2003**, *67*, 123512. [[CrossRef](#)]
44. Dimopoulos, K. Models of Quintessential Inflation. *arXiv* **2001**, arXiv:astro-ph/0111500.
45. Dimopoulos, K.; Valle, J.W.F. Modeling quintessential inflation. *Astropart. Phys.* **2002**, *18*, 287. [[CrossRef](#)]
46. Yahiro, M.; Mathews, G.J.; Ichiki, K.; Kajino, T.; Orito, M. Constraints on cosmic quintessence and quintessential inflation. *Phys. Rev. D* **2002**, *65*, 63502. [[CrossRef](#)]
47. Kaganovich, A.B. Field theory model giving rise to “quintessential inflation” without the cosmological constant and other fine-tuning problems. *Phys. Rev. D* **2000**, *63*, 25022. [[CrossRef](#)]
48. Baccigalupi, C.; Perrotta, F. Perturbations in quintessential inflation. *arXiv* **1998**, arXiv:astro-ph/9811385.
49. Lee, J.; Lee, T.H.; Oh, P.; Overduin, J. Cosmological coincidence without fine tuning. *Phys. Rev. D* **2014**, *90*, 123003. [[CrossRef](#)]
50. Capozziello, S.; Nojiri, S.; Odintsov, S.D. Unified phantom cosmology: Inflation, dark energy and dark matter under the same standard. *Phys. Lett. B* **2006**, *632*, 597–604. [[CrossRef](#)]
51. Nojiri, S.; Odintsov, S.D. Unifying phantom inflation with late-time acceleration: Scalar phantom–non-phantom transition model and generalized holographic dark energy. *Gen. Relativ. Grav.* **2006**, *38*, 1285. [[CrossRef](#)]
52. Elizalde, E.; Nojiri, S.; Odintsov, S.D.; Saez-Gomez, D.; Faraoni, V. Reconstructing the universe history, from inflation to acceleration, with phantom and canonical scalar fields. *Phys. Rev. D* **2008**, *77*, 106005. [[CrossRef](#)]
53. Hossain, M.W.; Myrzakulov, R.; Sami, M.; Saridakis, E.N. Class of quintessential inflation models with parameter space consistent with BICEP2. *Phys. Rev. D* **2014**, *89*, 123513. [[CrossRef](#)]
54. Guendelman, E.I.; Katz, O. Inflation and transition to a slowly accelerating phase from SSB of scale invariance. *Class. Quantum Grav.* **2003**, *20*, 1715. [[CrossRef](#)]
55. Hossain, M.W.; Myrzakulov, R.; Sami, M.; Saridakis, E.N. Unification of inflation and dark energy à la quintessential inflation. *Int. J. Mod. Phys. D* **2015**, *24*, 1530014. [[CrossRef](#)]
56. Ahmad, S.; Myrzakulov, R.; Sami, M. Relic gravitational waves from Quintessential Inflation. *Phys. Rev. D* **2017**, *96*, 63515. [[CrossRef](#)]
57. de Haro, J.; Saló, L.A. A Review of Quintessential Inflation. *Galaxies* **2021**, *9*, 73. [[CrossRef](#)]
58. Dimopoulos, K.; López, S.S. Quintessential inflation in Palatini  $f(R)$  gravity. *Phys. Rev. D* **2021**, *103*, 43533. [[CrossRef](#)]
59. Benisty, D.; Guendelman, E.I. Lorentzian Quintessential Inflation. *Int. J. Mod. Phys. D* **2020**, *29*, 2042002. [[CrossRef](#)]
60. Karčiauskas, M.; Rusak, S.; Saez, A. Quintessential Inflation and the Non-Linear Effects of the Tachyonic Trapping Mechanism. *arXiv* **2021**, arXiv:2112.11536.
61. Capozziello, S.; Carloni, S.; Troisi, A. Quintessence without scalar fields. *Recent Res. Dev. Astron. Astrophys.* **2003**, *1*, 625.
62. Sami, M.; Sahni, V. Quintessential inflation on the brane and the relic gravity wave background. *Phys. Rev. D* **2004**, *70*, 083513. [[CrossRef](#)]
63. Dimopoulos, K.; Owen, C. Quintessential Inflation with  $\alpha$ -attractors. *JCAP* **2017**, *6*, 27. [[CrossRef](#)]
64. Bettoni, D.; Rubio, J. Quintessential inflation: A tale of emergent and broken symmetries. *arXiv* **2021**, arXiv:2112.11948.
65. Dimopoulos, K.; Wood, L.D.; Owen, C. Instant preheating in quintessential inflation with  $\alpha$ -attractors. *Phys. Rev. D* **2018**, *97*, 63525. [[CrossRef](#)]
66. Wetterich, C. The quantum gravity connection between inflation and quintessence. *arXiv* **2022**, arXiv:2201.12213.
67. Jaman, N.; Myrzakulov, K. Braneworld inflation with an effective  $\alpha$ -attractor potential. *Phys. Rev. D* **2019**, *99*, 103523. [[CrossRef](#)]
68. Rosati, F. Quintessential enhancement of dark matter abundance. *Phys. Lett. B* **2003**, *570*, 5–10. [[CrossRef](#)]
69. Salati, P. Quintessence and the relic density of neutralinos. *Phys. Lett. B* **2003**, *571*, 121–131. [[CrossRef](#)]
70. Akrami, Y.; Kallosh, R.; Linde, A.; Vardanyan, V. Dark energy,  $\alpha$ -attractors, and large-scale structure surveys. *JCAP* **2018**, *6*, 41. [[CrossRef](#)]

71. Akrami, Y.; Casas, S.; Deng, S.; Vardanyan, V. Quintessential  $\alpha$ -attractor inflation: Forecasts for Stage IV galaxy surveys. *JCAP* **2021**, *4*, 6. [[CrossRef](#)]
72. Saba, N.; Farhoudi, M. Chameleon Field Dynamics During Inflation. *Int. J. Mod. Phys. D* **2017**, *27*, 1850041. [[CrossRef](#)]
73. Albrecht, A.; Steinhardt, P.J.; Turner, M.S.; Wilczek, F. Reheating an Inflationary Universe. *Phys. Rev. Lett.* **1982**, *48*, 1437. [[CrossRef](#)]
74. Dolgov, A.D.; Linde, A.D. Baryon Asymmetry in Inflationary Universe. *Phys. Lett. B* **1982**, *116*, 329. [[CrossRef](#)]
75. Abbott, L.F.; Farhi, E.; Wise, M.B. Particle Production in the New Inflationary Cosmology. *Phys. Lett. B* **1982**, *117*, 29. [[CrossRef](#)]
76. Ford, L.H. Gravitational Particle Creation and Inflation. *Phys. Rev. D* **1987**, *35*, 2955. [[CrossRef](#)]
77. Dolgov, A.D.; Kirilova, D.P. On particle creation by a time dependent scalar field. *Sov. J. Nucl. Phys.* **1990**, *51*, 172–177;
78. Traschen, J.H.; Brandenberger, R.H. Particle Production During Out-of-equilibrium Phase Transitions. *Phys. Rev. D* **1990**, *42*, 2491–2504. [[CrossRef](#)]
79. Spokoiny, B. Deflationary universe scenario. *Phys. Lett. B* **1993**, *315*, 40–45. [[CrossRef](#)]
80. Shtanov, Y.; Traschen, J.H.; Brandenberger, R.H. Universe reheating after inflation. *Phys. Rev. D* **1995**, *51*, 5438–5455. [[CrossRef](#)]
81. Kofman, L.; Linde, A.D.; Starobinsky, A.A. Reheating after inflation. *Phys. Rev. Lett.* **1994**, *73*, 3195–3198. [[CrossRef](#)] [[PubMed](#)]
82. Kofman, L.; Linde, A.D.; Starobinsky, A.A. Towards the theory of reheating after inflation. *Phys. Rev. D* **1997**, *56*, 3258–3295. [[CrossRef](#)]
83. Garcia-Bellido, J.; Linde, A.D. Preheating in hybrid inflation. *Phys. Rev. D* **1998**, *57*, 6075–6088. [[CrossRef](#)]
84. Felder, G.N.; Kofman, L.; Linde, A.D. Instant preheating. *Phys. Rev. D* **1999**, *59*, 123523. [[CrossRef](#)]
85. Lyth, D.H.; Wands, D. Generating the curvature perturbation without an inflaton. *Phys. Lett. B* **2002**, *524*, 5–14. [[CrossRef](#)]
86. Feng, B.; Li, M.Z. Curvaton reheating in nonoscillatory inflationary models. *Phys. Lett. B* **2003**, *564*, 169–174. [[CrossRef](#)]
87. del Campo, S.; Herrera, R.; Saavedra, J.; Campuzano, C.; Rojas, E. Curvaton reheating in logamediate inflationary model. *Phys. Rev. D* **2009**, *80*, 123531. [[CrossRef](#)]
88. Bassett, B.A.; Tsujikawa, S.; Wands, D. Inflation dynamics and reheating. *Rev. Mod. Phys.* **2006**, *78*, 537–589. [[CrossRef](#)]
89. Hardwick, R.J.; Vennin, V.; Koyama, K.; Wands, D. Constraining Curvaton Reheating. *JCAP* **2016**, *8*, 42. [[CrossRef](#)]
90. Campos, A.H.; Reis, H.C.; Rosenfeld, R. Preheating in quintessential inflation. *Phys. Lett. B* **2003**, *575*, 151–156. [[CrossRef](#)]
91. Allahverdi, R.; Brandenberger, R.; Cyr-Racine, F.Y.; Mazumdar, A. Reheating in Inflationary Cosmology: Theory and Applications. *Ann. Rev. Nucl. Part. Sci.* **2010**, *60*, 27–51. [[CrossRef](#)]
92. Amin, M.A.; Hertzberg, M.P.; Kaiser, D.I.; Karouby, J. Nonperturbative Dynamics Of Reheating After Inflation: A Review. *Int. J. Mod. Phys. D* **2014**, *24*, 1530003. [[CrossRef](#)]
93. Garcia, M.A.G.; Kaneta, K.; Mambriani, Y.; Olive, K.A. Reheating and Post-inflationary Production of Dark Matter. *Phys. Rev. D* **2020**, *101*, 123507. [[CrossRef](#)]
94. Tambalo, G.; Rinaldi, M. Inflation and reheating in scale-invariant scalar-tensor gravity. *Gen. Relativ. Gravit.* **2017**, *49*, 52. [[CrossRef](#)]
95. López, M.; Otalora, G.; Videla, N. Chaotic inflation and reheating in generalized scalar-tensor gravity. *JCAP* **2021**, *10*, 21. [[CrossRef](#)]
96. Saha, P. Model-independent constraints on inflation and reheating. *arXiv* **2021**, arXiv:2108.06612.
97. Pareek, P.; Nautiyal, A. Reheating constraints on k-inflation. *Phys. Rev. D* **2021**, *104*, 83526. [[CrossRef](#)]
98. Bhattacharya, S.; Das, K.; Gangopadhyay, M.R. Probing the era of reheating for reconstructed inflationary potential in the RS II braneworld. *Class. Quantum Gravity* **2020**, *37*, 215009. [[CrossRef](#)]
99. Dimopoulos, K.; Donaldson-Wood, L. Warm quintessential inflation. *Phys. Lett. B* **2019**, *796*, 26–31. [[CrossRef](#)]
100. Carroll, S.M.; Duvvuri, V.; Trodden, M.; Turner, M.S. Is cosmic speed-up due to new gravitational physics? *Phys. Rev. D* **2004**, *70*, 043528. [[CrossRef](#)]
101. Felice, A.D.; Tsujikawa, S.  $f(R)$  theories. *Living Rev. Relativ.* **2010**, *13*, 3. [[CrossRef](#)] [[PubMed](#)]
102. Sotiriou, T.P.; Faraoni, V.  $f(R)$  Theories Of Gravity. *Rev. Mod. Phys.* **2010**, *82*, 451–497. [[CrossRef](#)]
103. Gannouji, R.; Sami, M.; Thongkool, I. Generic  $f(R)$  theories and classicality of their scalarons. *Phys. Lett. B* **2012**, *716*, 255–259. [[CrossRef](#)]
104. Cosmai, L.; Fanizza, G.; Tedesco, L. Cosmic Acceleration and  $f(R)$  Theory: Perturbed Solution in a Matter FLRW Model. *Int. J. Theor. Phys.* **2016**, *55*, 754–765. [[CrossRef](#)]
105. Nojiri, S.; Odintsov, S.D. Modified non-local- $F(R)$  gravity as the key for the inflation and dark energy. *Phys. Lett. B* **2008**, *659*, 821–826. [[CrossRef](#)]
106. Dimopoulos, K.; Markkanen, T. Non-minimal gravitational reheating during kination. *JCAP* **2018**, *6*, 21. [[CrossRef](#)]
107. Bettoni, D.; Lopez-Eiguren, A.; Rubio, J. Hubble-induced phase transitions on the lattice with applications to Ricci reheating. *JCAP* **2022**, *1*, 2. [[CrossRef](#)]
108. Opferkuch, T.; Schwaller, P.; Stefanek, B.A. Ricci Reheating. *JCAP* **2019**, *7*, 16. [[CrossRef](#)]
109. Tashiro, H.; Chiba, T.; Sasaki, M. Reheating after quintessential inflation and gravitational waves. *Class. Quantum Gravity* **2004**, *21*, 1761–1772. [[CrossRef](#)]
110. Chun, E.J.; Scopel, S. Quintessential Kination and Leptogenesis. *JCAP* **2007**, *10*, 11. [[CrossRef](#)]
111. Kamada, K.; Kume, J.; Yamada, Y.; Yokoyama, J. Gravitational leptogenesis with kination and gravitational reheating. *JCAP* **2020**, *1*, 16. [[CrossRef](#)]

112. Berera, A.; Fang, L.Z. Thermally induced density perturbations in the inflation era. *Phys. Rev. Lett.* **1995**, *74*, 1912–1915. [[CrossRef](#)] [[PubMed](#)]
113. Berera, A. Warm inflation. *Phys. Rev. Lett.* **1995**, *75*, 3218–3221. [[CrossRef](#)]
114. Lima, G.B.F.; Ramos, R.O. Unified early and late Universe cosmology through dissipative effects in steep quintessential inflation potential models. *Phys. Rev. D* **2019**, *100*, 123529. [[CrossRef](#)]
115. Basak, S.; Bhattacharya, S.; Gangopadhyay, M.R.; Jaman, N.; Rangarajan, R.; Sami, M. The paradigm of warm quintessential inflation and spontaneous baryogenesis. *arXiv* **2021**, arXiv:2110.00607.
116. Levy, M.; Rosa, J.G.; Ventura, L.B. Warm inflation, neutrinos and dark matter: A minimal extension of the Standard Model. *JHEP* **2021**, *12*, 176. [[CrossRef](#)]
117. Gangopadhyay, M.R.; Myrzakul, S.; Sami, M.; Sharma, M.K. Paradigm of warm quintessential inflation and production of relic gravity waves. *Phys. Rev. D* **2021**, *103*, 43505. [[CrossRef](#)]
118. Ferreira, P.G.; Joyce, M. Structure formation with a selftuning scalar field. *Phys. Rev. Lett.* **1997**, *79*, 4740–4743. [[CrossRef](#)]
119. Ferreira, P.G.; Joyce, M. Cosmology with a primordial scaling field. *Phys. Rev. D* **1998**, *58*, 23503. [[CrossRef](#)]
120. Copeland, E.J.; Liddle, A.R.; Wands, D. Exponential potentials and cosmological scaling solutions. *Phys. Rev. D* **1998**, *57*, 4686–4690. [[CrossRef](#)]
121. Tsujikawa, S.; Sami, M. A unified approach to scaling solutions in a general cosmological background. *Phys. Lett. B* **2004**, *603*, 113–123. [[CrossRef](#)]
122. Steinhardt, P.J.; Wang, L.M.; Zlatev, I. Cosmological tracking solutions. *Phys. Rev. D* **1999**, *59*, 123504. [[CrossRef](#)]
123. Chiba, T. The Equation of State of Tracker Fields. *Phys. Rev. D* **2010**, *81*, 23515. [[CrossRef](#)]
124. Barreiro, T.; Copeland, E.J.; Nunes, N.J. Quintessence arising from exponential potentials. *Phys. Rev. D* **2000**, *61*, 127301. [[CrossRef](#)]
125. Haro, J.; Amorós, J.; Pan, S. Scaling solutions in quintessential inflation. *Eur. Phys. J. C* **2020**, *80*, 404. [[CrossRef](#)]
126. Tsujikawa, S.; Sami, M. String-inspired cosmology: A late time transition from a scaling matter era to a dark energy universe caused by a Gauss–Bonnet coupling. *JCAP* **2007**, *701*, 6. Pozdeeva, E.O.; Sami, M.; Toporensky, A.V.; Vernov, S.Y. *Phys. Rev. D* **2019**, *100*, 083527. [[CrossRef](#)]
127. Gumjudpai, B.; Naskar, T.; Sami, M.; Tsujikawa, S. Coupled dark energy: Towards a general description of the dynamics. *JCAP* **2005**, *6*, 7. [[CrossRef](#)]
128. Adhikari, R.; Gangopadhyay, M.R.; Yogesh. Power Law Plateau Inflation Potential In The RS II Braneworld Evading Swampland Conjecture. *Eur. Phys. J. C* **2020**, *80*, 899. [[CrossRef](#)]
129. Copeland, E.J.; Liddle, A.R.; Lidsey, J.E. Steep inflation: Ending brane world inflation by gravitational particle production. *Phys. Rev. D* **2001**, *64*, 23509. [[CrossRef](#)]
130. Geng, C.Q.; Hossain, M.W.; Myrzakulov, R.; Sami, M.; Saridakis, E.N. Quintessential inflation with canonical and noncanonical scalar fields and Planck 2015 results. *Phys. Rev. D* **2015**, *92*, 23522. [[CrossRef](#)]
131. Carroll, S.M. Why is the universe accelerating? In *AIP Conference Proceedings*; American Institute of Physics: College Park, MD, USA, 2004; Volume 743, pp. 16–32. [[CrossRef](#)]
132. Sahni, V. Dark matter and dark energy. In *The Physics of the Early Universe*; Lecture Notes in Physics; Springer: Berlin/Heidelberg, Germany, 2004; Volume 653, pp. 141–180. [[CrossRef](#)]
133. Sahni, V.; Starobinsky, A. Reconstructing Dark Energy. *Int. J. Mod. Phys. D* **2006**, *15*, 2105–2132. [[CrossRef](#)]
134. Mortonson, M.J.; Weinberg, D.H.; White, M. Dark Energy: A Short Review. *arXiv* **2013**, arXiv:1401.0046.
135. Sami, M.; Myrzakulov, R. Late time cosmic acceleration: ABCD of dark energy and modified theories of gravity. *Int. J. Mod. Phys. D* **2016**, *25*, 1630031. [[CrossRef](#)]
136. Copeland, E.J.; Sami, M.; Tsujikawa, S. Dynamics of dark energy. *Int. J. Mod. Phys. D* **2006**, *15*, 1753–1936. [[CrossRef](#)]
137. Li, M.; Li, X.D.; Wang, S.; Wang, Y. Dark Energy: A Brief Review. *Front. Phys.* **2013**, *8*, 828–846. [[CrossRef](#)]
138. Brax, P. What makes the Universe accelerate? A review on what dark energy could be and how to test it. *Rept. Prog. Phys.* **2018**, *81*, 16902. [[CrossRef](#)]
139. Zhang, Z. Geometrization of light bending and its application to SdS<sub>w</sub> spacetime. *Class. Quantum Gravity* **2022**, *39*, 15003. [[CrossRef](#)]
140. Ratra, B.; Peebles, P.J.E. Cosmological Consequences of a Rolling Homogeneous Scalar Field. *Phys. Rev. D* **1988**, *37*, 3406. [[CrossRef](#)]
141. Sami, M. Models of dark energy. In *The Invisible Universe: Dark Matter and Dark Energy*; Lecture Notes in Physics; Springer: Berlin/Heidelberg, Germany, 2007; Volume 720, pp. 219–256
142. Sami, M. A primer on problems and prospects of dark energy. *Curr. Sci.* **2009**, *97*, 887.
143. Akrami, Y.; Arroja, F.; Ashdown, M.; Aumont, J.; Baccigalupi, C.; Ballardini, M.; Banday, A.J.; Barreiro, R.B.; Bartolo, N.; Basak, S.; et al. Planck 2018 results. X. Constraints on inflation. *Astron. Astrophys.* **2020**, *641*, A10. [[CrossRef](#)]
144. Tristram, M.; Banday, A.J.; Górski, K.M.; Keskitalo, R.; Lawrence, C.R.; Andersen, K.J.; Barreiro, R.B.; Borrill, J.; Colombo, L.P.L.; Eriksen, H.K.; et al. Improved limits on the tensor-to-scalar ratio using BICEP and Planck. *arXiv* **2021**, arXiv:2112.07961.
145. Liddle, A.R.; Scherrer, R.J. A Classification of scalar field potentials with cosmological scaling solutions. *Phys. Rev. D* **1999**, *59*, 23509. [[CrossRef](#)]
146. Skugoreva, M.A.; Sami, M.; Jaman, N. Emergence of cosmological scaling behavior in the asymptotic regime. *Phys. Rev. D* **2019**, *100*, 43512. [[CrossRef](#)]

147. Kolb, E.W.; Turner, M.S. The Early Universe. *Front. Phys.* **1990**, *69*, 1–547. [[CrossRef](#)]
148. Husdal, L. On Effective Degrees of Freedom in the Early Universe. *Galaxies* **2016**, *4*, 78. [[CrossRef](#)]
149. Cyburt, R.H.; Fields, B.D.; Olive, K.A.; Yeh, T.H. Big Bang Nucleosynthesis: 2015. *Rev. Mod. Phys.* **2016**, *88*, 15004. [[CrossRef](#)]
150. Caprini, C.; Figueroa, D.G. Cosmological Backgrounds of Gravitational Waves. *Class. Quantum Gravity* **2018**, *35*, 163001. [[CrossRef](#)]
151. Cyburt, R.H.; Fields, B.D.; Olive, K.A.; Skillman, E. New BBN limits on physics beyond the standard model from  $^4\text{He}$ . *Astropart. Phys.* **2005**, *23*, 313–323. [[CrossRef](#)]
152. de la Macorra, A.; Piccinelli, G. Cosmological evolution of general scalar fields and quintessence. *Phys. Rev. D* **2000**, *61*, 123503. [[CrossRef](#)]
153. Nunes, A.; Mimoso, J.P. On the potentials yielding cosmological scaling solutions. *Phys. Lett. B* **2000**, *488*, 423–427. [[CrossRef](#)]
154. Ng, S.C.C.; Nunes, N.J.; Rosati, F. Applications of scalar attractor solutions to cosmology. *Phys. Rev. D* **2001**, *64*, 83510. [[CrossRef](#)]
155. Wetterich, C. Variable gravity Universe. *Phys. Rev. D* **2014**, *89*, 24005. [[CrossRef](#)]
156. Caldwell, R.R.; Linder, E.V. The Limits of quintessence. *Phys. Rev. Lett.* **2005**, *95*, 141301. [[CrossRef](#)] [[PubMed](#)]
157. Linder, E.V. The paths of quintessence. *Phys. Rev. D* **2006**, *73*, 63010. [[CrossRef](#)]
158. Scherrer, R.J.; Sen, A.A. Thawing quintessence with a nearly flat potential. *Phys. Rev. D* **2008**, *77*, 083515. [[CrossRef](#)]
159. Linder, E.V. Quintessence’s last stand? *Phys. Rev. D* **2015**, *91*, 63006. [[CrossRef](#)]
160. Urena-López, L.A.U.; Roy, N. Generalized tracker quintessence models for dark energy. *Phys. Rev. D* **2020**, *102*, 063510. [[CrossRef](#)]
161. Chiba, T. Slow-roll thawing quintessence. *Phys. Rev. D* **2009**, *79*, 083517, Erratum in *Phys. Rev. D* **2009**, *80*, 109902. [[CrossRef](#)]
162. Geng, C.; Lee, C.; Sami, M.; Saridakis, E.N.; Starobinsky, A.A. Observational constraints on successful model of quintessential Inflation. *JCAP* **2017**, *6*, 11. [[CrossRef](#)]
163. Scherrer, R.J. Exact general solutions for cosmological scalar field evolution in a background-dominated expansion. *arXiv* **2022**, arXiv:2202.01132.
164. Bartolo, N.; Pietroni, M. Scalar tensor gravity and quintessence. *Phys. Rev. D* **2000**, *61*, 23518. [[CrossRef](#)]
165. Saridakis, E.N.; Sushkov, S.V. Quintessence and phantom cosmology with non-minimal derivative coupling. *Phys. Rev. D* **2010**, *81*, 083510. [[CrossRef](#)]
166. Wetterich, C. Cosmon inflation. *Phys. Lett. B* **2013**, *726*, 15–22. [[CrossRef](#)]
167. Hossain, M.W.; Myrzakulov, R.; Sami, M.; Saridakis, E.N. Variable gravity: A suitable framework for quintessential inflation. *Phys. Rev. D* **2014**, *90*, 23512. [[CrossRef](#)]
168. Sami, M.; Gannouji, R. Spontaneous symmetry breaking in the late Universe and glimpses of the early Universe phase transitions à la baryogenesis. *Int. J. Mod. Phys. D* **2021**, *30*, 2130005. [[CrossRef](#)]
169. Sahni, V. The Energy Density of Relic Gravity Waves From Inflation. *Phys. Rev. D* **1990**, *42*, 453–463. [[CrossRef](#)]
170. Boyle, L.A.; Steinhardt, P.J. Probing the early universe with inflationary gravitational waves. *Phys. Rev. D* **2008**, *77*, 63504. [[CrossRef](#)]
171. Watanabe, Y.; Komatsu, E. Improved Calculation of the Primordial Gravitational Wave Spectrum in the Standard Model. *Phys. Rev. D* **2006**, *73*, 123515. [[CrossRef](#)]
172. Kuroyanagi, S.; Chiba, T.; Sugiyama, N. Precision calculations of the gravitational wave background spectrum from inflation. *Phys. Rev. D* **2009**, *79*, 103501. [[CrossRef](#)]
173. Ahmad, S.; Felice, A.D.; Jaman, N.; Kuroyanagi, S.; Sami, M. Baryogenesis in the paradigm of quintessential inflation. *Phys. Rev. D* **2019**, *100*, 103525. [[CrossRef](#)]
174. Figueroa, D.G.; Tanin, E.H. Inconsistency of an inflationary sector coupled only to Einstein gravity. *JCAP* **2019**, *10*, 50. [[CrossRef](#)]